Precision Physics at Colliders

HOW TO CHOOSE WISELY, MEASURE CAREFULLY, AND EXPLOIT RUTHLESSLY

Precision Physics at Colliders 2:

THE VISE OF ELECTROWEAK PRECISION

Theory vs. Experiment: Global Electroweak Fits

- Recall that the electroweak theory gauge boson sector has three independent parameters, e.g.:
  - GF, MZ, $\sin\theta_W$
  - g, g', v
  - and other ways
- The Higgs/Yukawa sector has many more: MH, fermion masses and mixings
- The high precision available experimentally in the gauge boson sector makes the observed effective masses and couplings accessible to higher-order radiative corrections.

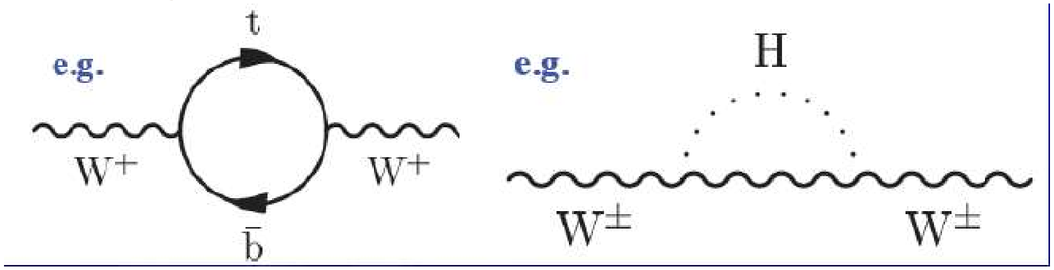

- This induces a non-trivial dependence between precision electroweak observables in the SM:
  - MW and MZ as effective physical observables now also have Mtop and MH dependence
  - $\sin\theta_W$ and other precision Z observables have different dependencies, which allows a global fit to constrain all of the underlying parameters.

Theory vs. Experiment: Global Electroweak Fits

arxiv:1803.01853

Measured ingredients:

MH, Mt

MW,MZ, ΓW, ΓZ

Partial widths of Z to heavy quarks, all hadrons, or leptons

Angular asymmetries of Z decays to fermions

Strong and electromagnetic couplings

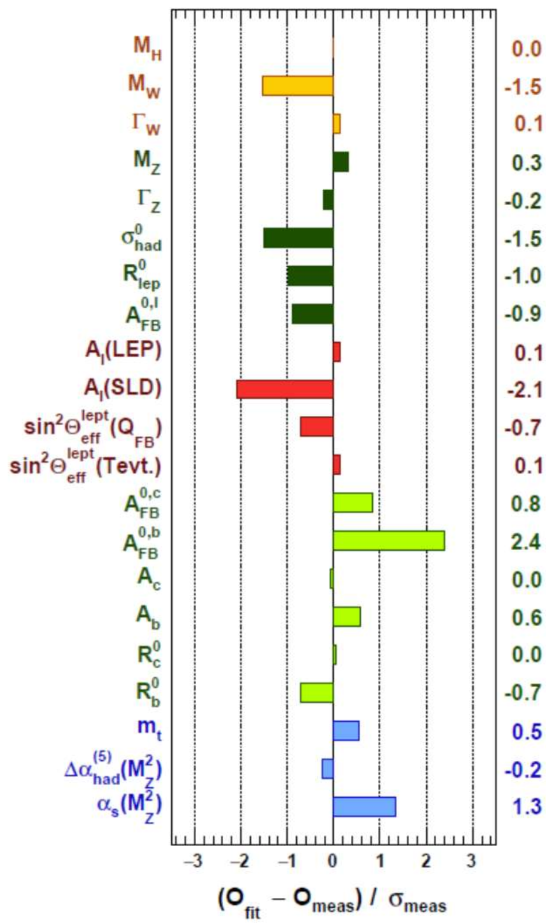

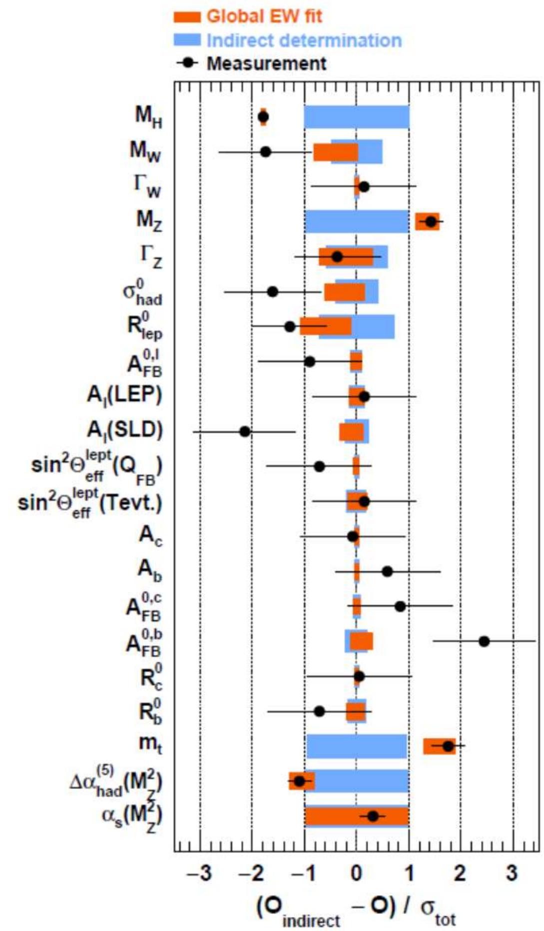

Theory vs. Experiment: Interpretation of fits

- A large "pull" tells you that the global fit prefers a different value than observed.
- If the measurement disagrees with the prediction obtained from all of the other measurements (Indirect determination) that indicates a theory inconsistency.
- A dramatic enough difference is evidence of BSM phenomena participating in the radiative corrections (or we need more sophisticated SM predictions)

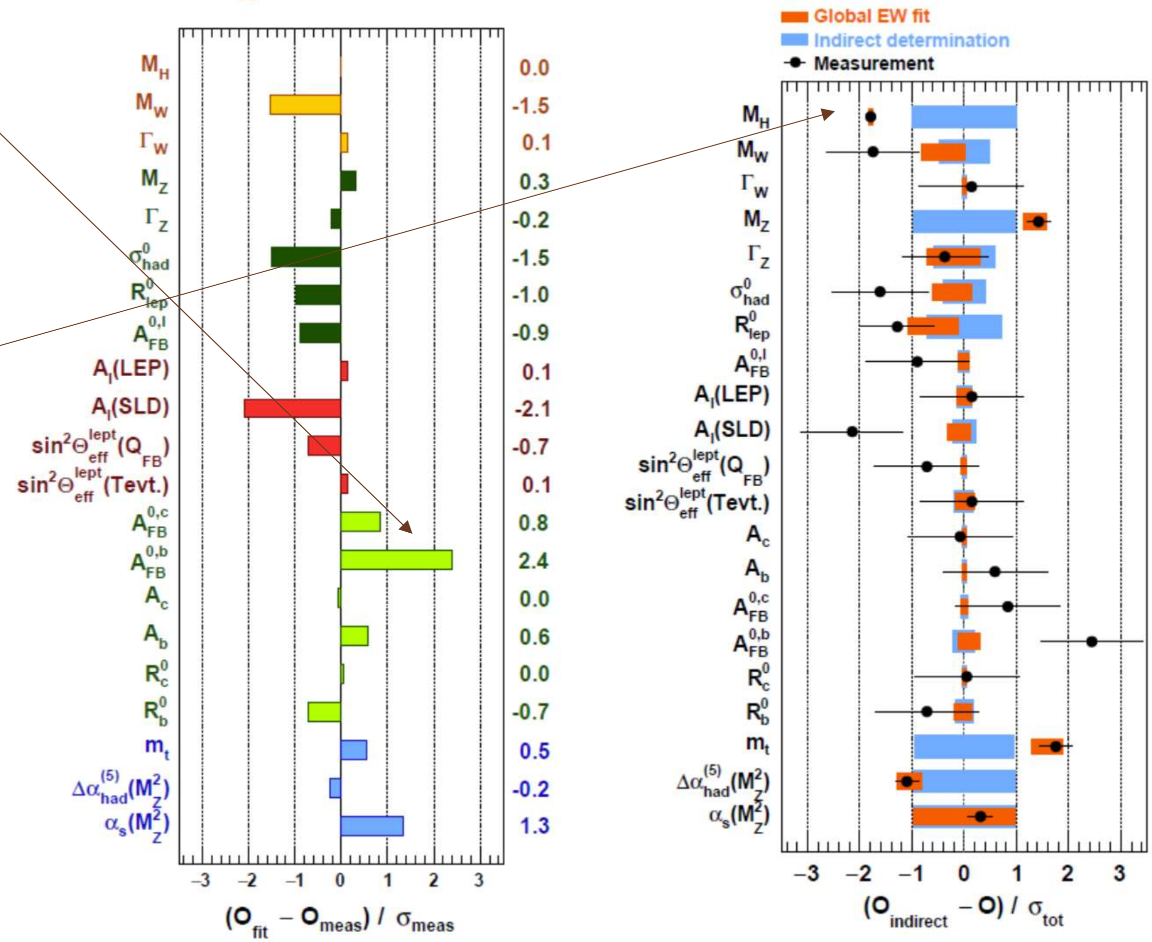

Theory vs. Experiment: Mt and MH hunting

Historically, this has been used to predict Mt and MH before they were discovered!

Mt, MW, MH interrelation was the most popular way to track this.

Mt and MH are now so well-measured that higher precision has minimal impact on the indirect determination of the others!

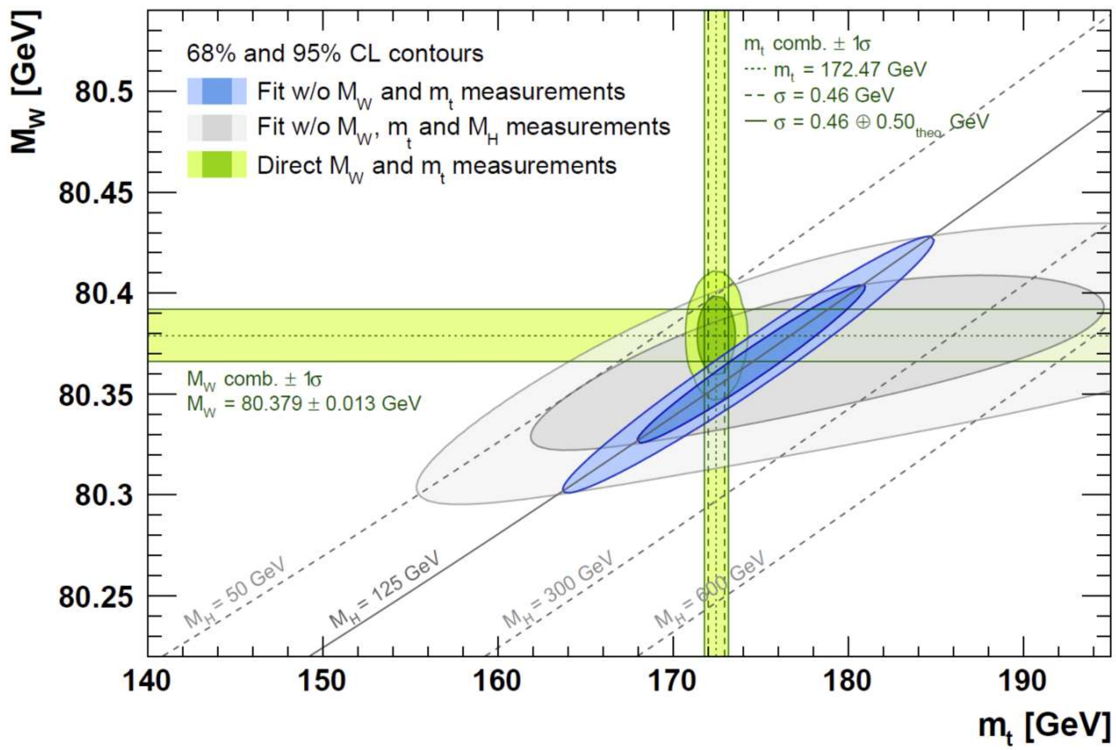

Theory vs. Experiment: Time for W and Z to catch up

What measurements will tighten the vise with the next 2X in precision?

The W mass is now better known indirectly (blue) than directly (points), and its improvement will affect the global chi2.

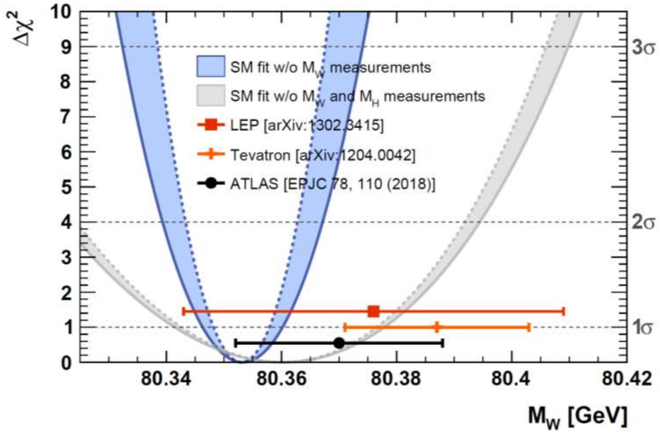

Similarly, **the weak mixing angle** is in a similar state, and would benefit from a third opinion to resolve the discrepancy between LEP and SLD.

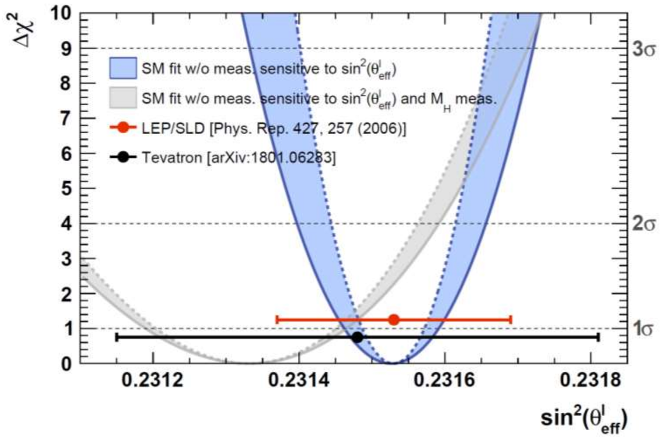

Resolving AFB_b will probably require ILC/FCC-ee/CepC ☹

The weak mixing angle at hadron colliders

$q\bar{q} \rightarrow Z/\gamma^* \rightarrow ll$ differential cross section at LO:

$$\frac{d\sigma}{dy^{\ell\ell}\, dm^{\ell\ell}\, d\cos\theta} = \frac{3}{16\pi} \frac{d\sigma^{U+L}}{dy^{\ell\ell}\, dm^{\ell\ell}} \left\{ (1 + \cos^2\theta) + A_4 \cos\theta \right\}$$

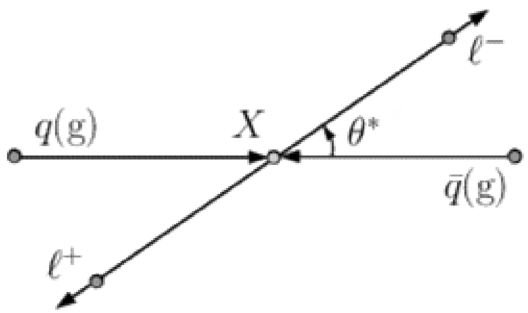

- In the di-lepton CM, lepton angle with respect to axis of quark momentum is sensitive to interference effects: vector with axial-vector Z couplings, Z with photon (or Z with new physics)

- The A4 term odd in cos θ^* is very sensitive to the weak mixing angle when M = MZ.

- The odd term coefficient A4 can be obtained from an angular fit or computed from the forward-backward asymmetry

AFB = $(\sigma(\cos\theta^*>0) - \sigma(\cos\theta^*<0))/\sigma$
= $3/8 * A4$

How to measure the scattering angle

- Unlike a lepton collider, we cannot perfectly divine the incoming fermion/anti-fermion directions.
  - For non-zero PT, cannot identify "which" incoming parton radiated
- PT effect is minimized by choosing the Collins-Soper frame
- For l- four vector P1, l+ four vector P2:

$$\cos\theta^*_{CS} = \frac{2(P_1^+ P_2^- - P_1^- P_2^+)}{\sqrt{Q^2(Q^2+Q_T^2)}} \qquad P_i^{\pm} = (E_i \pm P_{z,i})/\sqrt{2}$$

Q = P1+P2

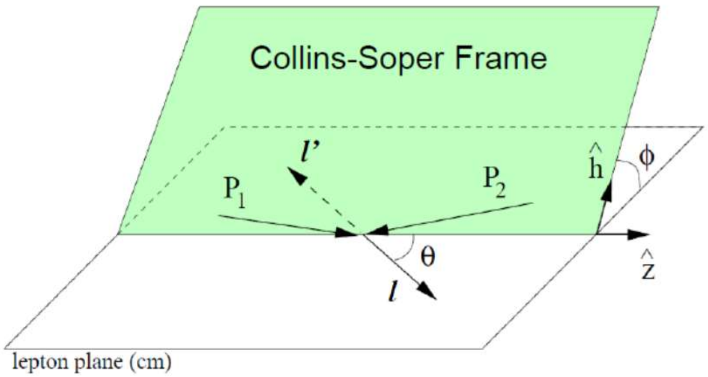

In dilepton CM frame:
z-axis bisects proton1 and –proton2 angle,
x-axis is Z PT direction

How to measure the scattering angle

- Unlike a lepton collider, we cannot perfectly divine the incoming fermion/anti-fermion directions.
    - Which proton (or antiproton) originates the quark or antiquark is ambiguous

- The parton ambiguity is unavoidable, and there is a parton-dependent dilution to the ideal case.
- At the Tevatron, valence quark/anti-valence quark annihilation dominates, therefore the proton carries the quark a very large fraction of the time.

- At LHC, Z production is predominantly valence quark-sea quark annihilation
- The valence quark usually carries more of the proton momentum, so the Z Pz direction is correlated with the quark direction

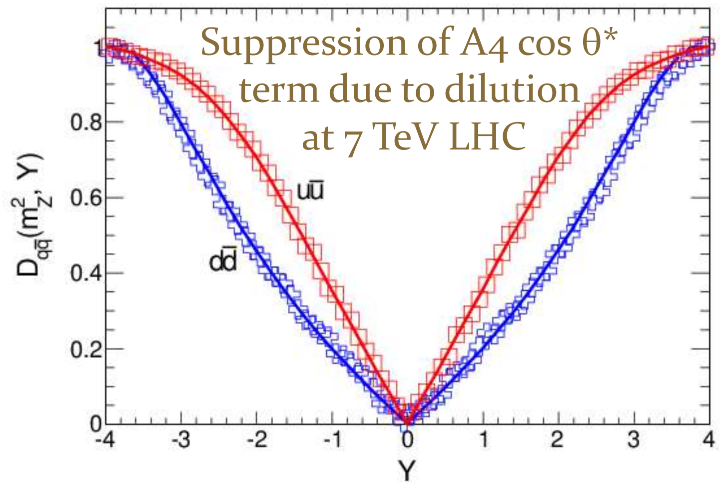

The more forward the Z production the less ambiguous the quark direction is

SM behavior of AFB and the weak mixing angle

- The weak mixing angle sensitivity arises from the Z vector and axial-vector coupling diagrams self-interfering, giving a small positive AFB of a few percent. The photon diagram also interferes with the Z, giving very large effects above and below the Z pole.

- Virtual electroweak corrections modify the LO relation between A4 and $\sin^2\theta_W$, leading to an "effective" mixing angle as the baseline observable:

$$\frac{v_l}{a_l} = 1 - 4 \cdot K_Z^\ell \cdot \sin^2\theta_W \Rightarrow \sin^2\theta_{\mathrm{eff}}^\ell = K_Z^\ell \cdot \sin^2\theta_W$$

- A4 ~ ¼ - $\sin^2\theta_{\mathrm{eff}}$, so

A4 precision of 0.001 → mixing angle precision of 20×10^{-5}

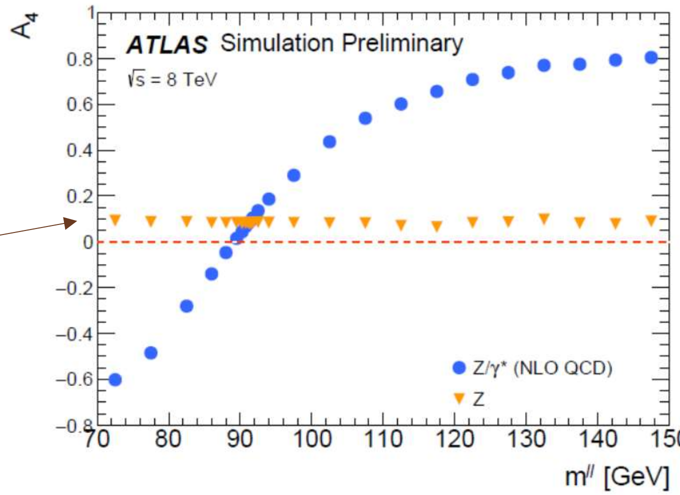

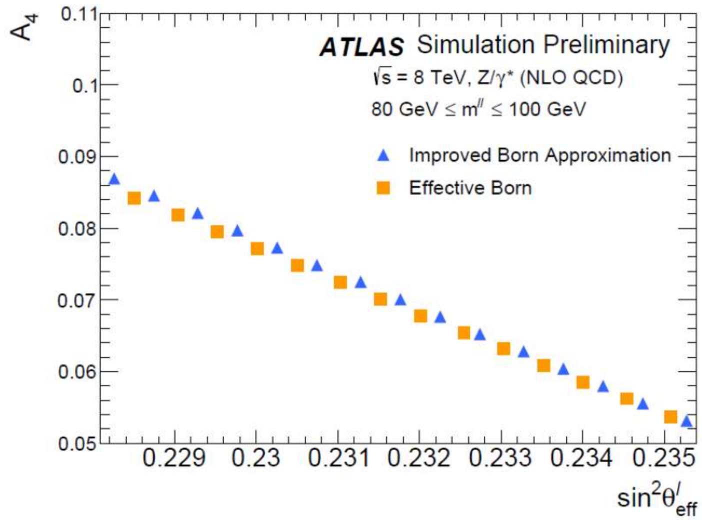

A4 measurement strategy

- At NNLO QCD, up to 9 different non-zero angular terms to consider including A4.
- Dilepton PT dependence is especially hard to model, so integrate that out
- For several bins of y and m, construct 8x8 bin templates for each of the 9 angular polynomials, modified for detector acceptance and higher-order corrections to the baseline MC (POWHEG-BOX), i.e, a four-dimensional histogram.
- Differential dilepton data along with nuisance parameters are included in a grand likelihood hit to determine A4.

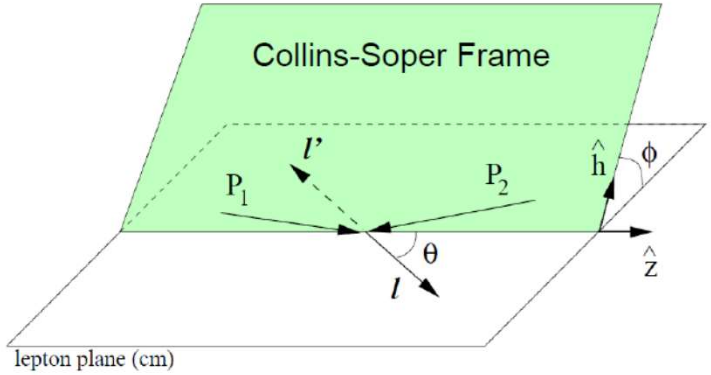

$$\frac{d\sigma}{dp_T^{\ell\ell}\, dy^{\ell\ell}\, dm^{\ell\ell}\, d\cos\theta\, d\phi} = \frac{3}{16\pi}\frac{d\sigma^{U+L}}{dp_T^{\ell\ell}\, dy^{\ell\ell}\, dm^{\ell\ell}}$$
$$\Big\{(1+\cos^2\theta) + \frac{1}{2} A_0(1-3\cos^2\theta) + A_1 \sin 2\theta \cos\phi$$
$$+\frac{1}{2} A_2 \sin^2\theta \cos 2\phi + A_3 \sin\theta \cos\phi + A_4 \cos\theta$$
$$+A_5 \sin^2\theta \sin 2\phi + A_6 \sin 2\theta \sin\phi + A_7 \sin\theta \sin\phi\Big\}$$

Likelihood fit design

1280 bins in (m, y) x θ x ϕ = 20x8x8

Nuisance priors

$$\mathcal{L}(A,\sigma,\theta|N_{\rm obs}) = \prod_{n}^{N_{\rm bins}} \left\{P(N^n_{\rm obs}|N^n_{\rm exp}(A,\sigma,\theta))P(N^n_{\rm eff}|\gamma^n N^n_{\rm eff})\right\} \times \prod_{m}^{M} G(0|\beta^m,1)$$

Poisson probability for data Nobs

Poisson probability for template MC Neff

$$N^n_{\rm exp}(A,\sigma,\theta) = \left\{\sum_{j=0}^{\rm N_{bins}} \sigma_j \times L \times \left[t^n_{8j}(\beta) + \sum_{i=0}^{7} A_{ij} \times t^n_{ij}(\beta)\right]\right\} \times \gamma^n + \sum_{B}^{\rm bkgs} T^n_B(\beta)$$

Cross section x lumi in bin j

Ang. Coeff. i in bin j

9 angular templates for bin j and their nuisance parameter dependence

Backgrounds and their nuisance parameter dependence

$$A_{4,j}(\sin^2\theta^{\ell}_{\rm eff},\ \theta) = a_j(\theta) \times \sin^2\theta^{\ell}_{\rm eff} + b_j(\theta)$$

A4 mixing angle dependence (linear interpolation in each bin j, w/nuisances)

Event selection and categorization

- ee_{CC} : two electrons in the central tracking and calorimetry (|η|<2.4)
  - 12 GeV dielectron trigger
  - 25 GeV PT requirement of =2 opposite sign electrons
- $\mu\mu_{CC}$: two muons in the central tracking and muon systems (|η|<2.4)
  - 24 GeV single muon trigger
  - 25 GeV PT requirement of =2 opposite sign muons
- ee_{CF} : one electron in central tracking/calorimetry (|η|<2.4), one in **endcap/forward calorimetry** (2.5 < |η| < 4.9)
  - 24 GeV single central electron trigger
  - 25/20 GeV C/F PT requirement with tighter ID than ee_{CC}

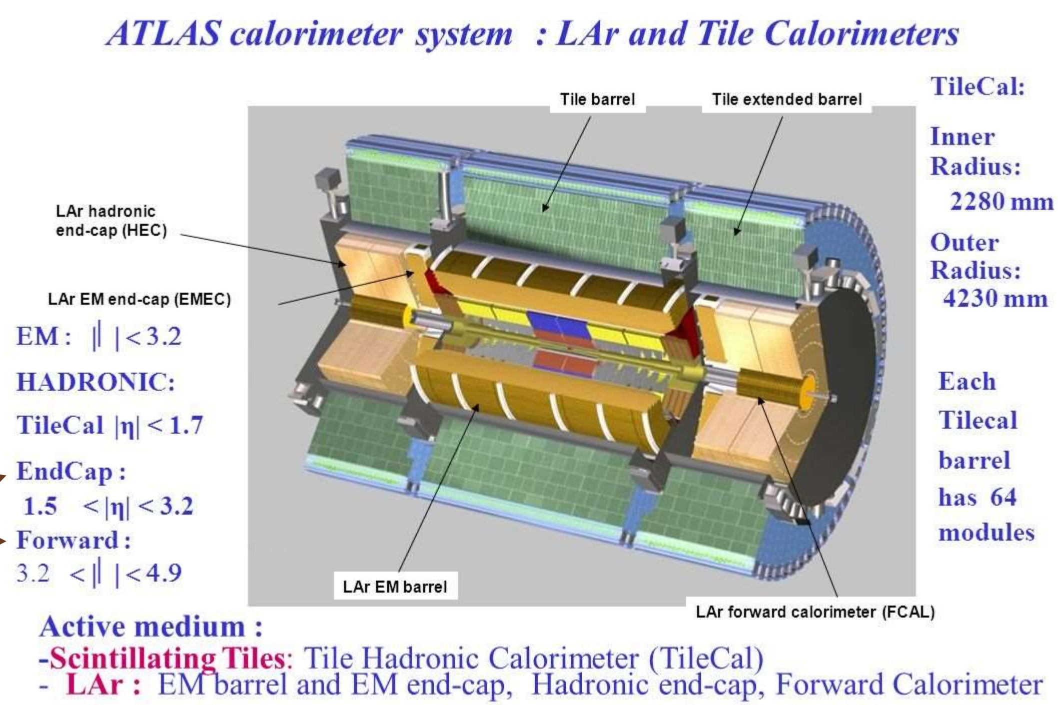

Event selection and categorization

- ee_{CC} : two electrons in the central tracking and calorimetry (|η|<2.4)
  - 12 GeV di-electron trigger
  - 25 GeV PT requirement of =2 opposite sign electrons
- $\mu\mu_{CC}$: two muons in the central tracking and muon systems (|η|<2.4)
  - 24 GeV single muon trigger
  - 25 GeV PT requirement of =2 opposite sign muons

- ee_{CF} : one electron in central tracking/calorimetry (|η|<2.4), one in **endcap/forward calorimetry** (2.5 < |η| < 4.9)
  - 24 GeV single central electron trigger
  - 25/20 GeV C/F PT requirement with tighter ID than ee_{CC}

1. ee_{CC} and $\mu\mu_{CC}$:
   - three bins in m_{ll} with bin boundaries {70, 80, 100, 125} in GeV,
   - three bins in $|y_{ll}|$ with bin boundaries {0, 0.8, 1.6, 2.5};
2. ee_{CF}:
   - one bin in m_{ll} with bin boundaries {80, 100} in GeV,
   - two bins in $|y_{ll}|$ with bin boundaries {1.6, 2.5, 3.6}.

About 6-7M events each for CC categories, 1M for CF

	$80 < m_{ll} < 100$ GeV			
$\lvert y_{ll}\rvert$	Data	Top+EW	Multijets	Non-fiducial Z
1.6-2.5	702 142	0.001	0.010	0.017
2.5-3.6	441 104	0.001	0.011	0.013

Pre-fit angular distributions

- Data/MC agreement for $\mu\mu_{CC}$ and ee_{CF} in the Z pole mass region for all y.
- Only a small raw AFB is visible for CC; a larger one emerges for CF, as expected.
- S/B at the Z pole is very high
- cos2ϕ modulation from A2 can be clearly seen

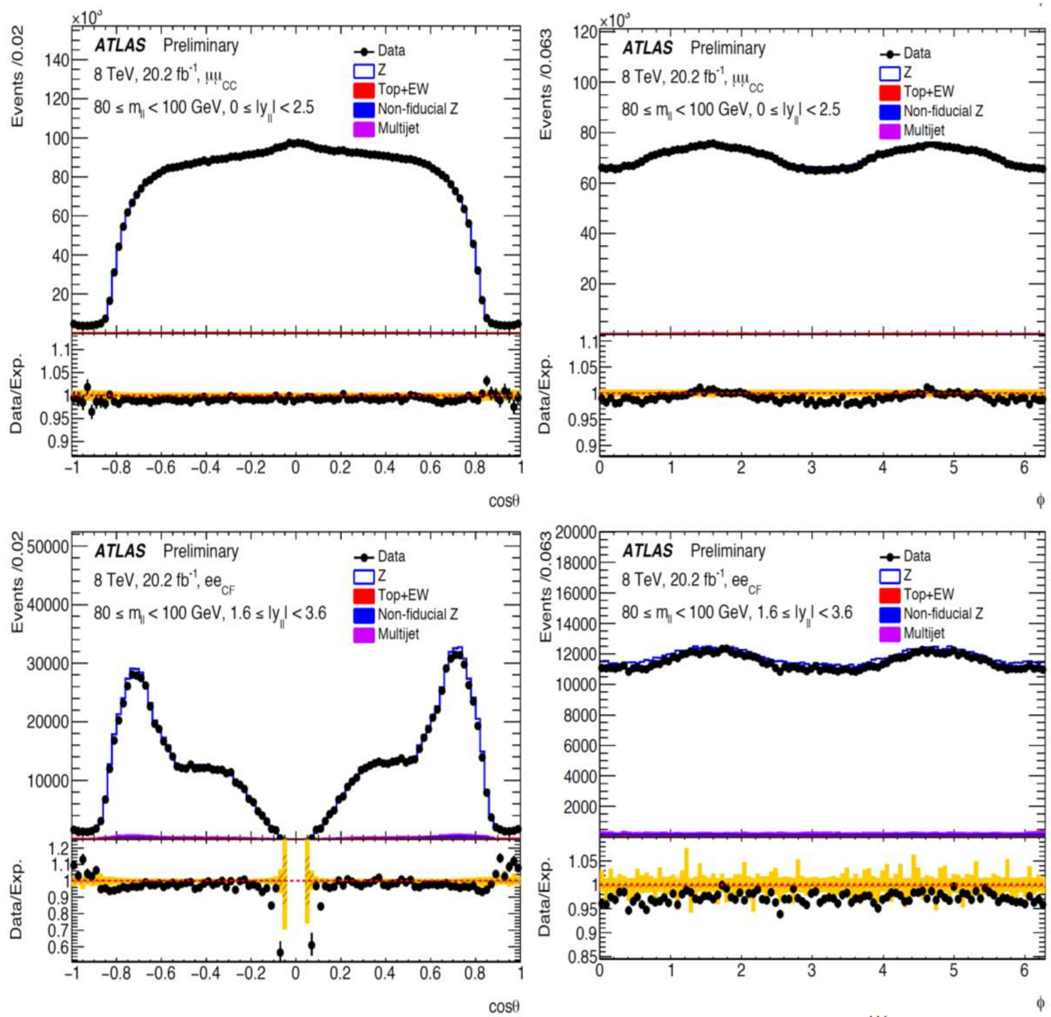

Fit results and uncertainties

- Consistent results for all three categories
- ee_{CF} is as powerful as $ee_{CC}+\mu\mu_{CC}$
- All three categories systematics limited, predominantly by PDF uncertainty affecting relation between A4 and mixing angle

Channel	ee_{CC}	$\mu\mu_{CC}$	ee_{CF}	$ee_{CC}+\mu\mu_{CC}$	$ee_{CC}+\mu\mu_{CC}+ee_{CF}$
Central value	0.23148	0.23123	0.23166	0.23119	0.23140
	Uncertainties				
Total	68	59	43	49	36
Stat.	48	40	29	31	21
Syst.	48	44	32	38	29
	Uncertainties in measurements				
PDF (meas.)	8	9	7	6	4
p_T^Z modelling	0	0	7	0	5
Lepton scale	4	4	4	4	3
Lepton resolution	6	1	2	2	1
Lepton efficiency	11	3	3	2	4
Electron charge misidentification	2	0	1	1	< 1
Muon sagitta bias	0	5	0	1	2
Background	1	2	1	1	2
MC. stat.	25	22	18	16	12
	Uncertainties in predictions				
PDF (predictions)	37	35	22	33	24
QCD scales	6	8	9	5	6
EW corrections	3	3	3	3	3

Internal consistency across categories

- Using eeCF outermost bin as a reference, compute pulls of other categories
- Innermost CC Z pole category is an outlier, others are consistent

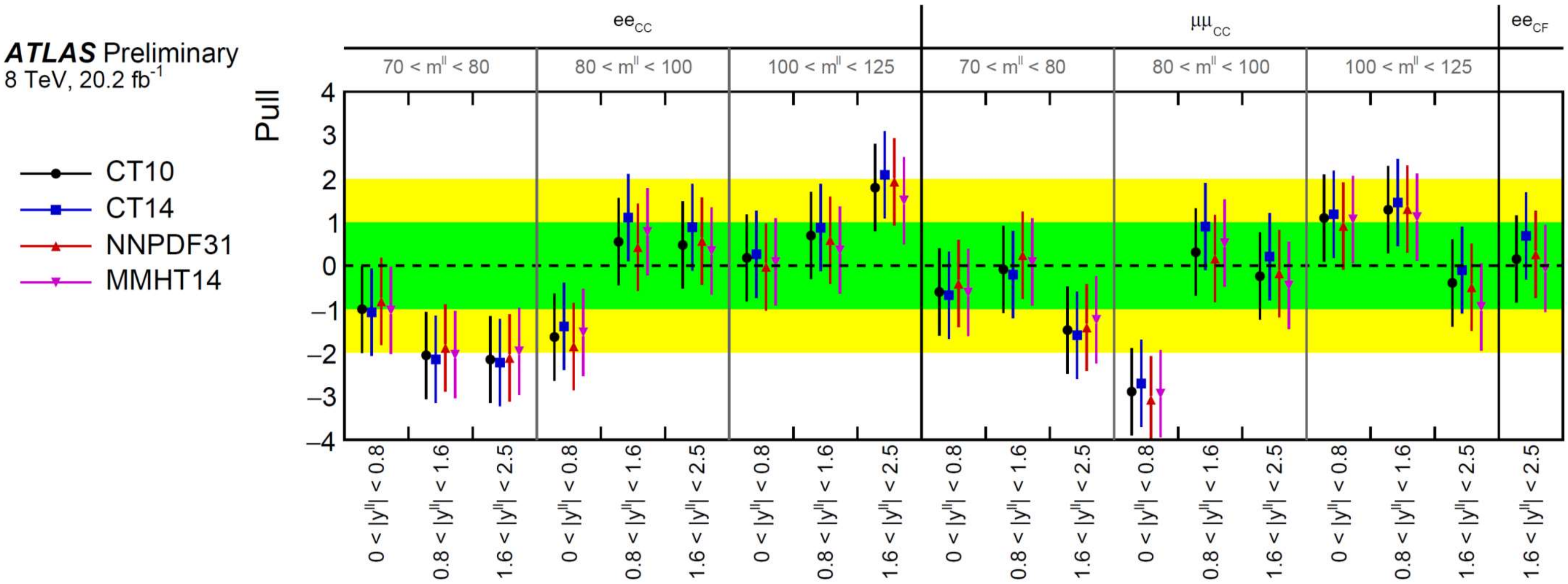

Comparison with ROTW

- About 2.2X less precise than LEP/SLD
- Comparable to Tevatron final results
- Superior to CMS 8 TeV, which does not include ee_{CF} category.
- Superior to LHCb due to luminosity/statistics (LHCb has lower PDF unc.!)

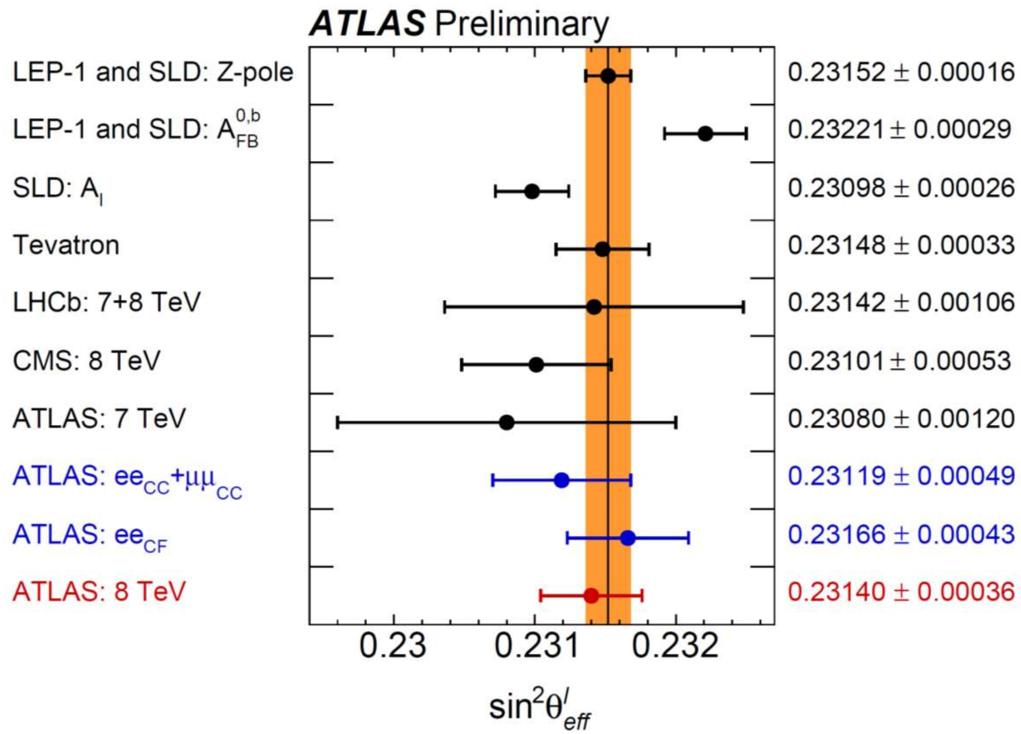

$$0.23140 \pm 0.00021\ (\text{stat.}) \pm 0.00024\ (\text{PDF}) \pm 0.00016\ (\text{syst.})$$

Uncertainty analysis, prospects for 13 TeV

- Systematics limited (29 vs. 21 E-5 stat. unc.)

- Affects of PDF uncertainties on $\sin^2\theta_{eff}$(A4) predominate (24E-5)
  - Admixture of partons determines A4 dilution
  - External improvement or simultaneous constraint with more data needed to improve upon this!
  - These unfortunately worsen at 13 TeV

- Stat (21) and MC stat (12) unc. will improve together with 13 TeV data

- QCD scales improvement will need beyond NNLO (!) prediction

- PTZ modelling with data can be introduced to ee_{CF} sample with larger datasets.

Channel	$ee_{CC} + \mu\mu_{CC} + ee_{CF}$
Central value	0.23140
Total	36
Stat.	21
Syst.	29
PDF (meas.)	4
p_T^Z modelling	5
Lepton scale	3
Lepton resolution	1
Lepton efficiency	4
Electron charge misidentification	< 1
Muon sagitta bias	2
Background	2
MC. stat.	12
PDF (predictions)	24
QCD scales	6
EW corrections	3

The mass of the W boson

- In the electroweak theory, α, GF, MZ, MW related at tree-level via a simple algebraic relation. With radiative corrections Δr, there is also a dependence on Mt and MH at high precision.

$$M_{\mathrm{W}}^2 = M_{\mathrm{Z}}^2 \left\{ \frac{1}{2} + \sqrt{\frac{1}{4} - \frac{\pi\alpha}{\sqrt{2} G_\mu M_{\mathrm{Z}}^2} \left[1 + \Delta r(M_{\mathrm{W}}, M_{\mathrm{Z}}, M_{\mathrm{H}}, m_{\mathrm{t}}, \ldots) \right]} \right\}$$

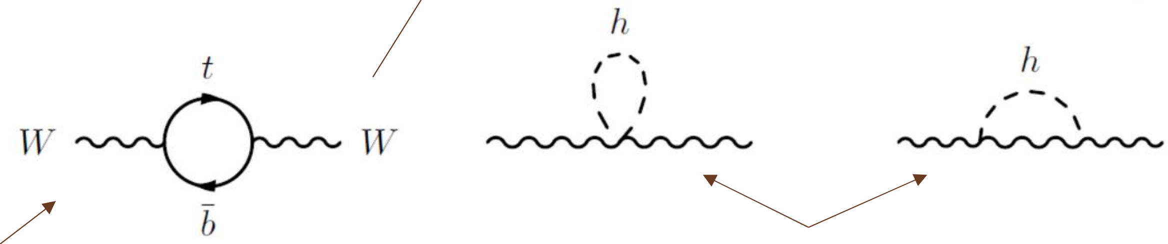

$$\Delta r_{SM}^t = -\frac{G_\mu}{\sqrt{2}} \frac{N_c}{8\pi^2} \left(\frac{c_W^2}{s_W^2} \right) m_t^2 + \log(m_t) \text{ terms}$$

$$\Delta r_{SM}^h \sim \frac{\alpha}{\pi s_W^2} \frac{11}{48} \log\left(\frac{m_h^2}{M_Z^2} \right) + \mathcal{O}\left(\frac{m_h^2}{M_Z^2}, \frac{v^4}{\Lambda^4} \right)$$

New fermions or bosons coupling to W can shift observed MW from SM predictions 10's of MeV

W production at the LHC

- Two main experimental observables are the lepton transverse momentum and the transverse momentum of everything recoiling against it

$$\vec{p}_{\mathrm{T}}^{\ell} \qquad \vec{u}_{\mathrm{T}} = \sum_i \vec{E}_{\mathrm{T},i}$$

- It is useful to analyze uT in components parallel and perpendicular to the lepton. The neutrino transvers momentum is inferred from –vector sum

$$\vec{p}_{\mathrm{T}}^{\mathrm{miss}} = -\left(\vec{p}_{\mathrm{T}}^{\ell} + \vec{u}_{\mathrm{T}}\right)$$

- Invariant mass cannot be measured directly. The "transverse mass" mT can be computed in the transverse plane, with a kinematic edge terminating at MW.

- Lepton PT alone has great resolution and its distribution (peaking at MW/2) is a good estimator of MW, but has strong dependence on W PT modelling.

- MT has much weaker W PT dependence, but has worse resolution from Ptmiss. Let's measure both!

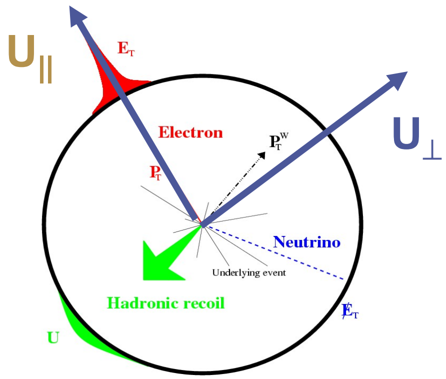

$$m_T = \sqrt{2 p_T^{\,l} p_T^{\,\nu} (1 - \cos\phi_{l\nu})}$$

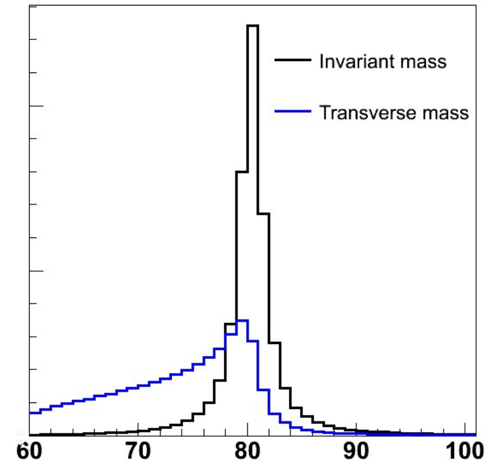

W production at the LHC

- W production is majority valence quark/sea anti-quark annihilation, but at least 1/3 is from sea quark/sea anti-quark of various flavors.
- The proton has twice as many ups as downs, so W+ cross section is higher than W-, and the kinematics and PDF dependence differ
- Higher rapidity → stronger valence quark component → better known PDFs. Charge and rapidity dependence of PDFs motivates a binned MW analysis.
- W PT is predominantly less than 30 GeV, where theory prediction relies critically on soft gluon resummation.
- Production model is sensitive to sea quark distribution of the different flavors, including heavy flavor combinations not probed by the Z (cs, cb)

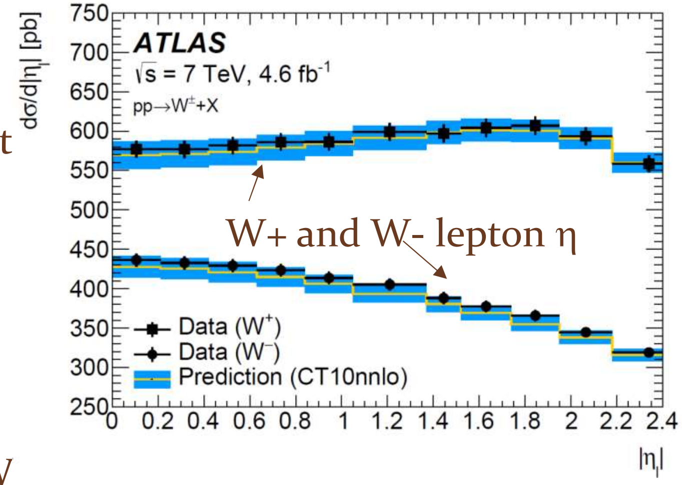

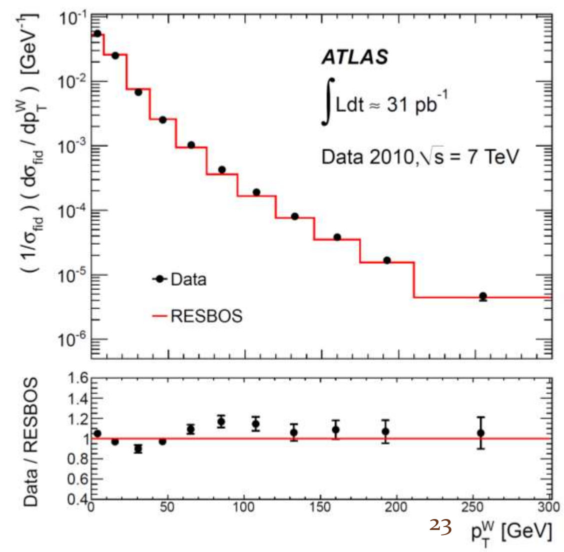

Event selection and categorization

- W selection
  - Single muon trigger with 18 GeV PT OR single electron trigger with 20-22 GeV PT

$$p_T^\ell > 30\text{ GeV} \quad p_T^{\text{miss}} > 30\text{ GeV} \quad u_T < 30\text{ GeV} \quad m_T > 60\text{ GeV}$$

  - Measure leptons out to a pseudo-rapidity of 2.4.
  - **6M W → enu, 8M W→ munu selected in 4.1-4.6 /fb at 7 TeV**
  - Electron channel has 2% background from W → taunu, Z →ee, 0.4% other
  - Muon channel has 6% background from W/Z, 0.3% other
- Z selection: 2 opposite sign leptons with PT > 25 GeV (0.6M ee, 1.2M μμ)

- Categorize **by lepton, charge, and rapidity**. Measure MW separately from 1D templates of MT and PT, and combine with correlations (~50% correlated)

Decay channel	$W \to e\nu$	$W \to \mu\nu$
Kinematic distributions	p_T^ℓ, m_T	p_T^ℓ, m_T
Charge categories	W^+, W^-	W^+, W^-
$\lvert\eta_\ell\rvert$ categories	[0, 0.6], [0.6, 1.2], [1.8, 2.4]	[0, 0.8], [0.8, 1.4], [1.4, 2.0], [2.0, 2.4]

Electron energy scale calibration

- ATLAS EM calorimetry consists of 3 depth layers of LAr
  - L1 has high-granularity η strips for lateral shape, L2 has larger square cells and most of the X0, L3 is a tail catcher
  - Preshower detector in the barrel estimates pre-radiation upstream
- Simulation-based response corrections
- Electron and unconverted photon longitudinal response studied to correct the upstream material model
- Minimum-ionizing muons are used to intercalibrate different depth layers and analyze crosstalk

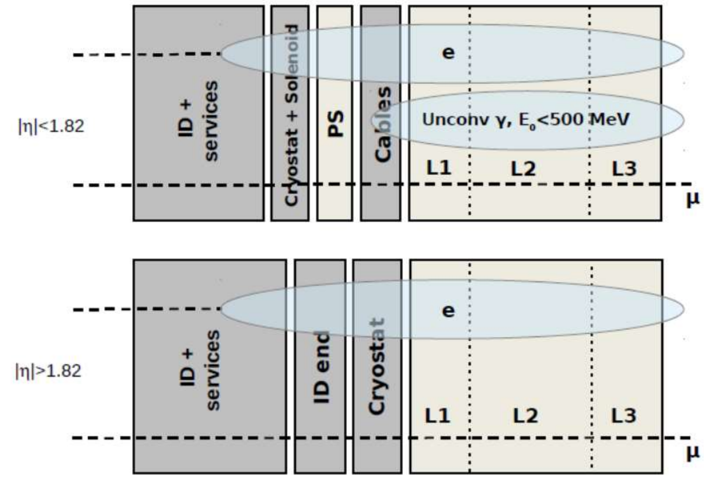

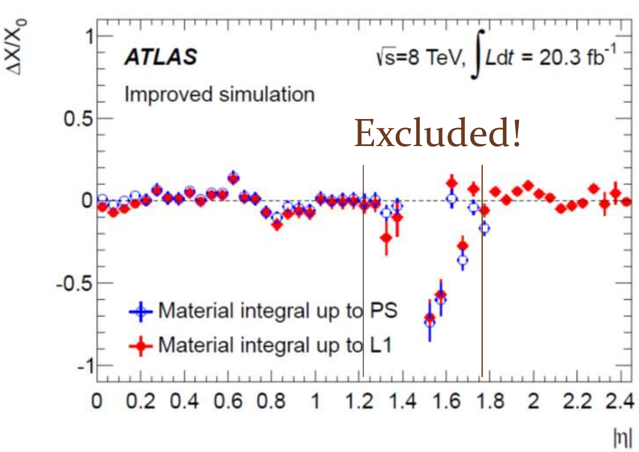

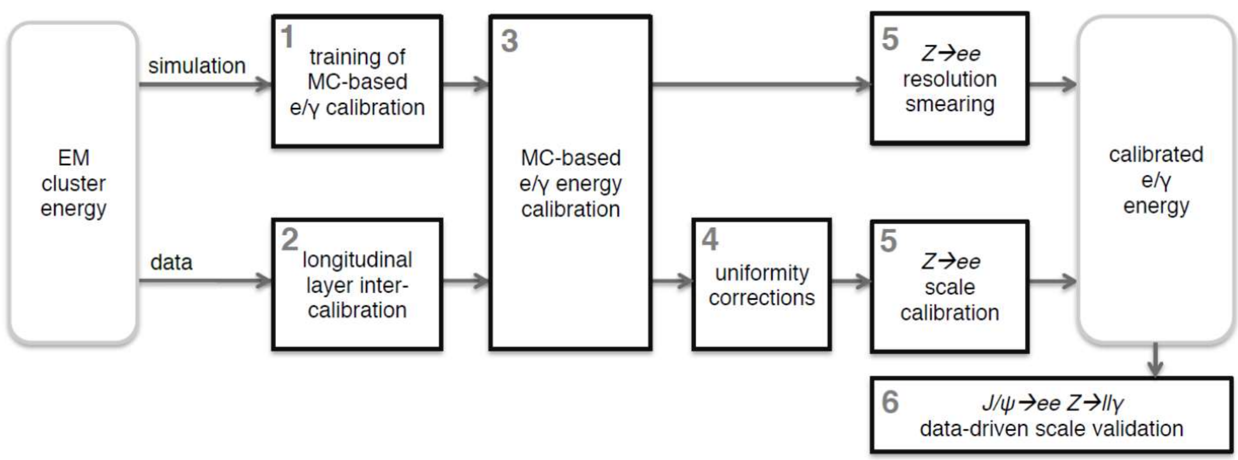

Electron energy scale calibration

- Residual data-driven corrections obtained from W electrons, J/psi or Z di-electron data.
- Azimuthal distortions (mechanical sagging, e.g.) corrected with E/p relative corrections

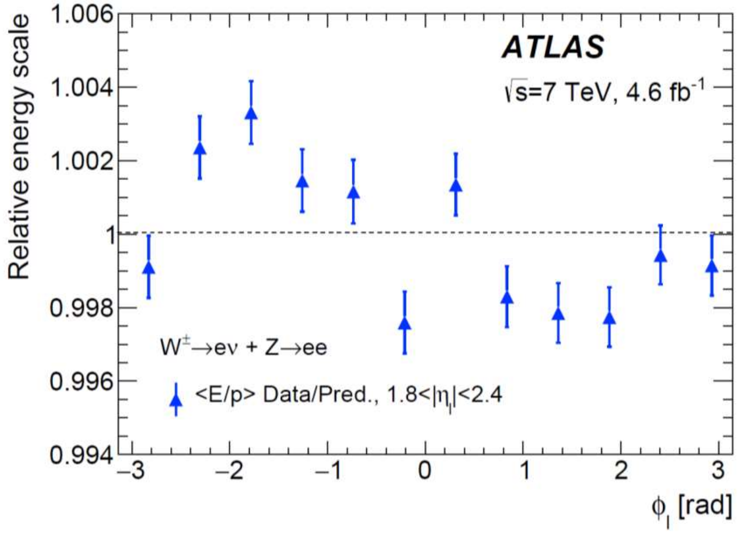

- Energy scale vs. h calibrated to center the Z mass at the expected value
- Resolution simultaneously adjusted to match the observed linewidth

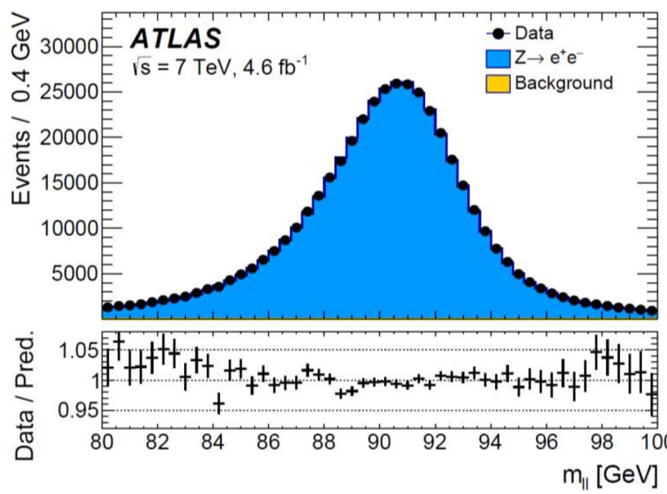

Electron efficiency calibration

- Z → ee data also used to estimate efficiency corrections (tag and probe method)
- Resulting corrected MC η distribution matches the data

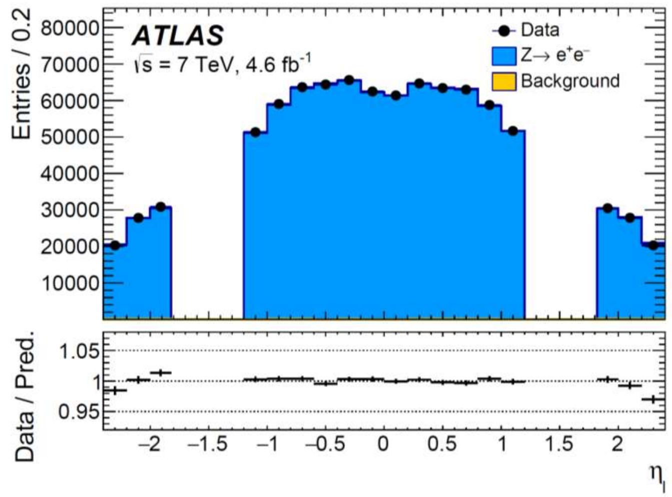

- Energy scale, efficiency corrections have largest impact on MW
- Resolution also important at high η

$\|\eta_\ell\|$ range	[0.0, 0.6]		[0.6, 1.2]		[1.82, 2.4]		Combined	
Kinematic distribution	p_T^ℓ	m_T	p_T^ℓ	m_T	p_T^ℓ	m_T	p_T^ℓ	m_T
δm_W [MeV]								
Energy scale	10.4	10.3	10.8	10.1	16.1	17.1	8.1	8.0
Energy resolution	5.0	6.0	7.3	6.7	10.4	15.5	3.5	5.5
Energy linearity	2.2	4.2	5.8	8.9	8.6	10.6	3.4	5.5
Energy tails	2.3	3.3	2.3	3.3	2.3	3.3	2.3	3.3
Reconstruction efficiency	10.5	8.8	9.9	7.8	14.5	11.0	7.2	6.0
Identification efficiency	10.4	7.7	11.7	8.8	16.7	12.1	7.3	5.6
Trigger and isolation efficiencies	0.2	0.5	0.3	0.5	2.0	2.2	0.8	0.9
Charge mismeasurement	0.2	0.2	0.2	0.2	1.5	1.5	0.1	0.1
Total	19.0	17.5	21.1	19.4	30.7	30.5	14.2	14.3

Muon momentum scale calibration

- Muon momentum is determined by the ATLAS Inner Detector tracking
- Three classes of biases to correct for
  - α(η,ϕ): momentum scale
  - β(η): intrinsic resolution (radial)
  - δ(η,ϕ): sagitta (twists or curls)

$$p_{\mathrm{T}}^{\mathrm{MC,corr}} = p_{\mathrm{T}}^{\mathrm{MC}} \times [1+\alpha(\eta,\phi)] \times \left[1+\beta_{\mathrm{curv}}(\eta)\cdot G(0,1)\cdot p_{\mathrm{T}}^{\mathrm{MC}}\right]$$

$$p_{\mathrm{T}}^{\mathrm{data,corr}} = \frac{p_{\mathrm{T}}^{\mathrm{data}}}{1+q\cdot\delta(\eta,\phi)\cdot p_{\mathrm{T}}^{\mathrm{data}}},$$

- α,β, and δ can be calibrated to the observed Z → μμ mass

- Linear extrapolation estimated for α to calibrate MW PT range (**dominant uncertainty, δPT/PT = 2-7 x 10-4**)

- δ independently estimated from W→eν E/p mean behavior, exploiting charge-independence of E

$$\delta_{\mathrm{sagitta}} = (<E/p>^{+} - <E/p>^{-})/2\times <E_{\mathrm{T}}>$$

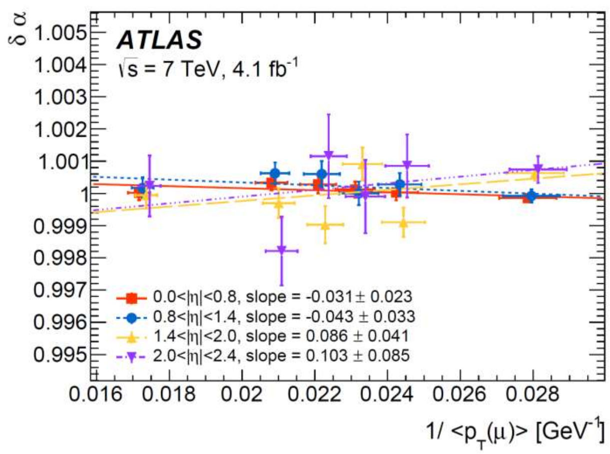

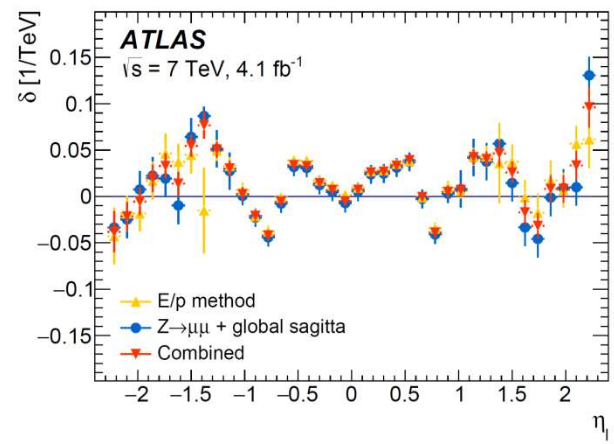

Muon efficiency calibration

- Z di-muon data calibrates efficiencies
- Binned in PT and η

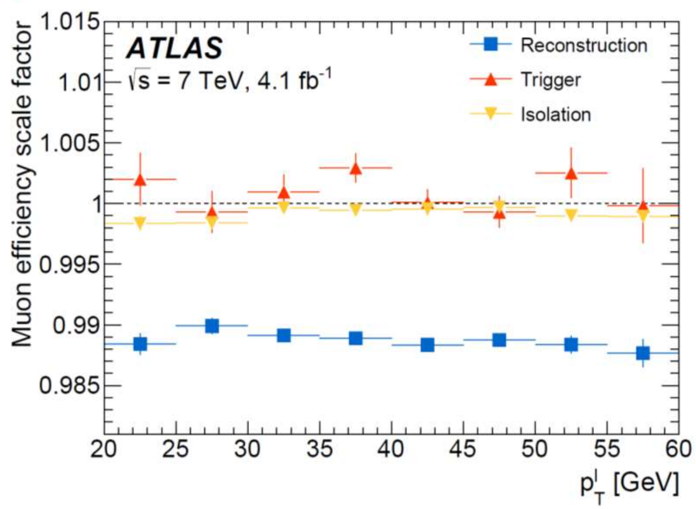

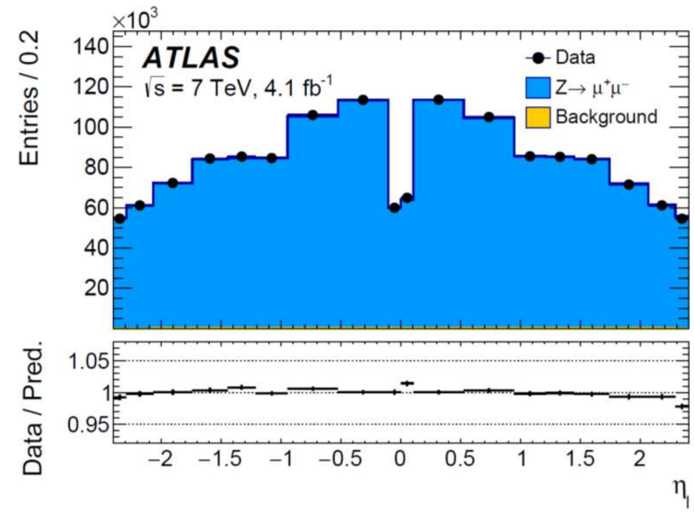

- Momentum scale, trigger efficiency corrections have largest impact on MW

$\lvert\eta_\ell\rvert$ range	[0.0, 0.8]		[0.8, 1.4]		[1.4, 2.0]		[2.0, 2.4]		Combined	
Kinematic distribution	p_T^ℓ	m_T	p_T^ℓ	m_T	p_T^ℓ	m_T	p_T^ℓ	m_T	p_T^ℓ	m_T
δm_W [MeV]										
Momentum scale	8.9	9.3	14.2	15.6	27.4	29.2	111.0	115.4	8.4	8.8
Momentum resolution	1.8	2.0	1.9	1.7	1.5	2.2	3.4	3.8	1.0	1.2
Sagitta bias	0.7	0.8	1.7	1.7	3.1	3.1	4.5	4.3	0.6	0.6
Reconstruction and isolation efficiencies	4.0	3.6	5.1	3.7	4.7	3.5	6.4	5.5	2.7	2.2
Trigger efficiency	5.6	5.0	7.1	5.0	11.8	9.1	12.1	9.9	4.1	3.2
Total	11.4	11.4	16.9	17.0	30.4	31.0	112.0	116.1	9.8	9.7

Recoil calibration

- Mean pileup in simulation is adjusted to the observed distribution.
- Simulated recoil sumET distribution for Z is transformed into the observed one via Smirnov transform (transforming x to match the CDFs).

- The simulated W recoil sumET is then transformed similarly to match the data-driven estimate

$$\tilde{h}^W(\Sigma\bar{E}_\mathrm{T}, p_\mathrm{T}^W) \equiv h^Z_\mathrm{data}(\Sigma\bar{E}_\mathrm{T}, p_\mathrm{T}^{\ell\ell})\left(\frac{h^W_\mathrm{data}(\Sigma\bar{E}_\mathrm{T})}{h^W_\mathrm{MC}(\Sigma\bar{E}_\mathrm{T})} \bigg/ \frac{h^Z_\mathrm{data}(\Sigma\bar{E}_\mathrm{T})}{h^Z_\mathrm{MC}(\Sigma\bar{E}_\mathrm{T})}\right)$$

- Azimuthal anisotropies in recoil are corrected to match Z → μμ data

$$\begin{aligned} u'_x &= u_x + (\langle u_x\rangle_\mathrm{data} - \langle u_x\rangle_\mathrm{MC}) \\ u'_y &= u_y + (\langle u_y\rangle_\mathrm{data} - \langle u_y\rangle_\mathrm{MC}) \end{aligned}$$

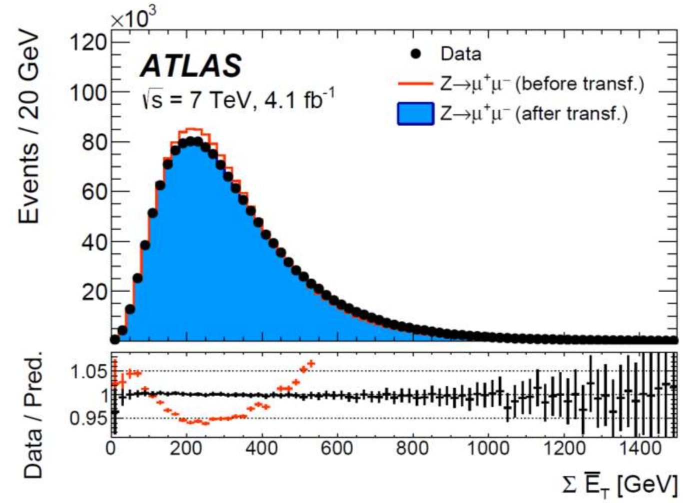

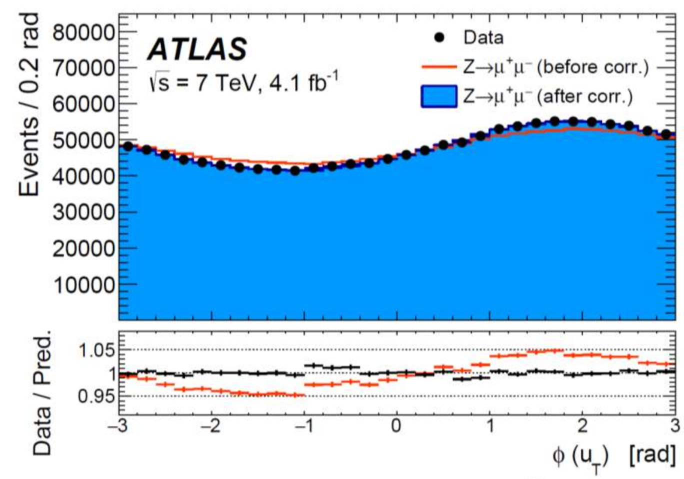

Recoil calibration

- Residual correction of uperp and u|| needed to agree with data
- Z PT data precisely estimates these components

$$u_{\parallel}^{V,\mathrm{corr}} = u_{\parallel}^{V,\mathrm{MC}} + b(p_{\mathrm{T}}^{V}, \Sigma \bar{E}_{\mathrm{T}}{}') + (u_{\parallel}^{V,\mathrm{MC}} + p_{\mathrm{T}}^{V}) \cdot r(p_{\mathrm{T}}^{V}, \Sigma \bar{E}_{\mathrm{T}}{}')$$
$$u_{\perp}^{V,\mathrm{corr}} = u_{\perp}^{V,\mathrm{MC}} \cdot r(p_{\mathrm{T}}^{V}, \Sigma \bar{E}_{\mathrm{T}}{}'),$$

- b additively corrects the mean difference in response scale of $u_{\parallel}^{Z} + p_{\mathrm{T}}^{\ell\ell}$
- r multiplicatively corrects the response resolution
- Correction binned in pileup, V PT, and sumET to create a response model for W

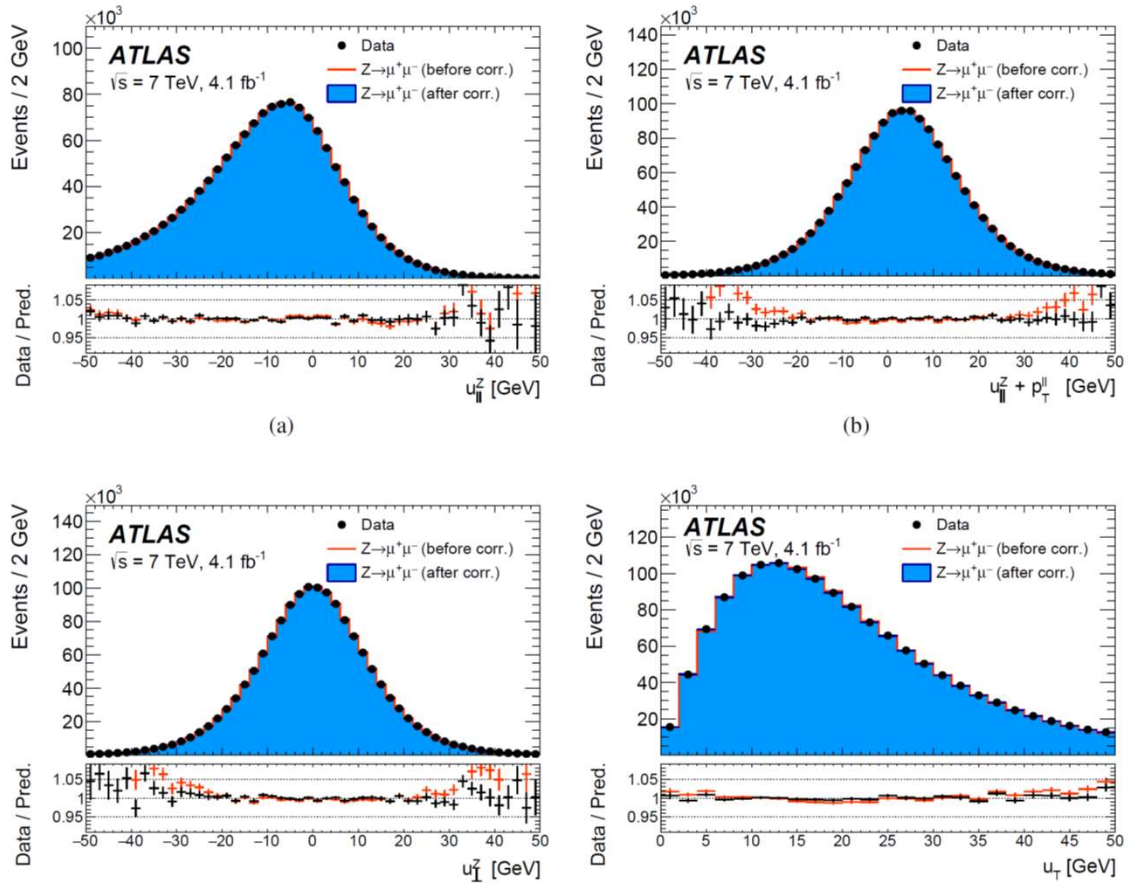

Recoil calibration

- As a closure test, this procedure can successfully transform POWHEG+HERWIG6 into POWHEG+PYTHIA8

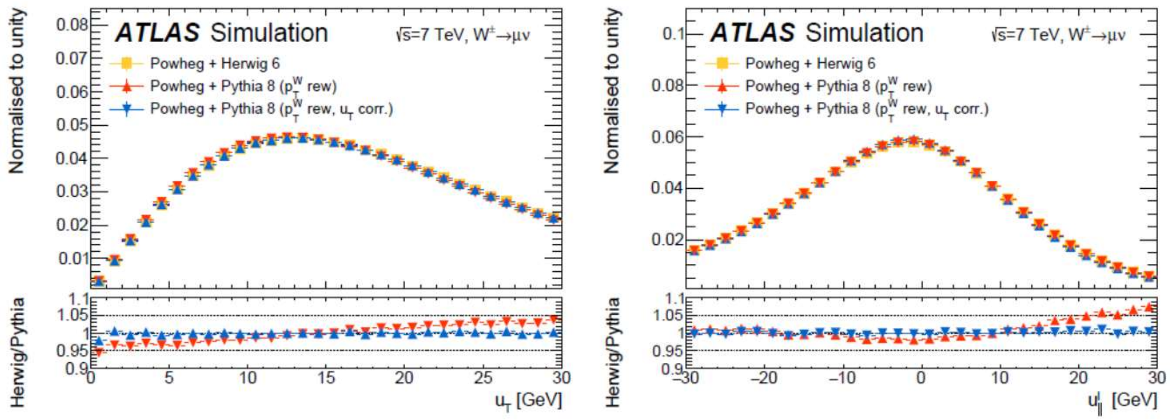

- Dominant systematic is the sumET correction: difference between correction binned in PT or performed inclusively is 10 MeV

W-boson charge	W^+		W^-		Combined	
Kinematic distribution	p_T^ℓ	m_T	p_T^ℓ	m_T	p_T^ℓ	m_T
δm_W [MeV]						
$\langle\mu\rangle$ scale factor	0.2	1.0	0.2	1.0	0.2	1.0
$\Sigma\bar{E}_T$ correction	0.9	12.2	1.1	10.2	1.0	11.2
Residual corrections (statistics)	2.0	2.7	2.0	2.7	2.0	2.7
Residual corrections (interpolation)	1.4	3.1	1.4	3.1	1.4	3.1
Residual corrections ($Z \to W$ extrapolation)	0.2	5.8	0.2	4.3	0.2	5.1
Total	2.6	14.2	2.7	11.8	2.6	13.0

Building a signal template

- 5-dimensional model with all-order effects included is not available at this time!
- Relevant factors are built up separately from data and MCs

$$\frac{d\sigma}{dp_1\, dp_2} = \left[\frac{d\sigma(m)}{dm}\right]\left[\frac{d\sigma(y)}{dy}\right]\left[\frac{d\sigma(p_T, y)}{dp_T\, dy}\left(\frac{d\sigma(y)}{dy}\right)^{-1}\right]\left[(1+\cos^2\theta) + \sum_{i=0}^{7} A_i(p_T, y) P_i(\cos\theta, \phi)\right]$$

Boson mass | Boson rapidity | Normalized PT and y | Normalized angular dist.

- Mass is a **relativistic Breit-Wigner distribution** (with width recomputed vs. mass…); Z boson case includes photon diagram and interference

$$\frac{d\sigma}{dm} \propto \frac{m^2}{(m^2 - m_V^2)^2 + m^4\Gamma_V^2/m_V^2}$$

- Rapidity and angular distributions are estimated from **fixed-order NNLO calculations (DYNNLO)**
- PT estimation requires resummed soft-gluon emission and non-perturbative effects. **PYTHIA 8 + PS** with some re-tunings used to predict this (in agreement with dedicated NLO+PS and resummed calculations).
- Fully simulated+corrected POWHEG+PYTHIA8, w/AZNLO tune and CT10 PDF, is reweighted to match these.

Building a signal template: V PT

- PYTHIA 8 has 3 parameters to tune PS showering
  - Intrinsic parton PT
  - Strong coupling for ISR
  - ISR infrared cutoff

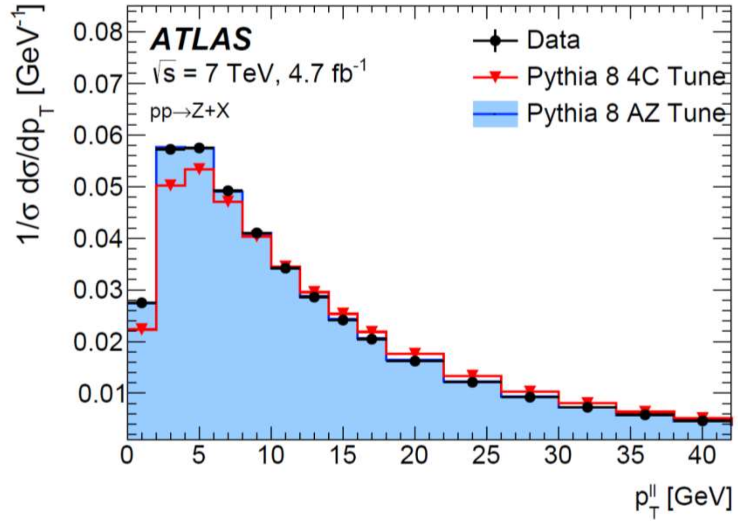

- "AZ tune" gave the best description of 7 TeV data; other tunes, NLO+PS, and resummed predictions did not agree well with data and give big variations in lepton PT.

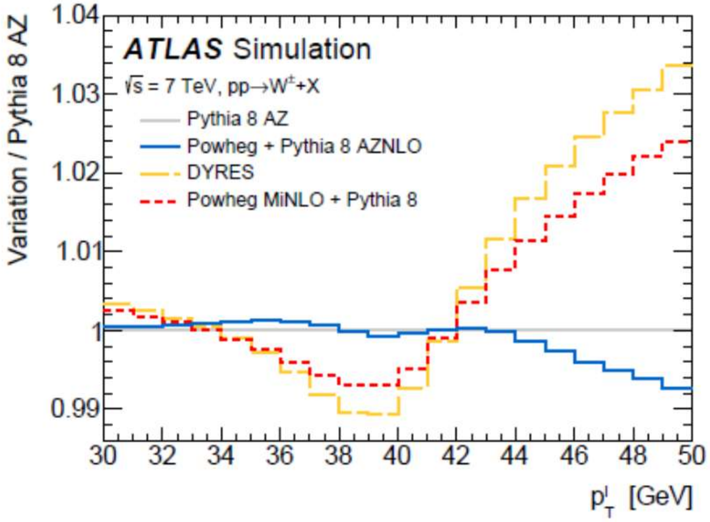

AZ tune also describes well the measured W PT/Z PT ratio

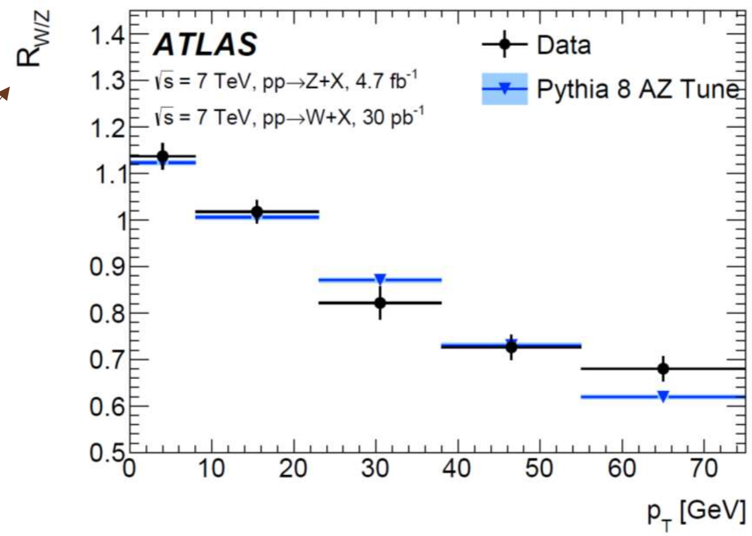

W template systematic uncertainties

- PDF uncertainty in the templates has the largest impact on MW (8-9 MeV)

- CT10NNLO PDF is the baseline. Its Hessian error matrix has 25 error eigenvectors which can be varied independently. All 25 +/- variations are used to regenerate or reweight each piece of the signal template.

- Combining charges reduces PDF uncertainty due to anti-correlated u-sea and d-sea!
- Similarly, binning by lepton rapidity also reduces PDF uncertainty.
- MMHT14 and CT14NNLO are also used to bound the uncertainty (4 MeV)

W-boson charge	W^+		W^-		Combined	
Kinematic distribution	p_T^ℓ	m_T	p_T^ℓ	m_T	p_T^ℓ	m_T
δm_W [MeV]						
Fixed-order PDF uncertainty	13.1	14.9	12.0	14.2	8.0	8.7
AZ tune	3.0	3.4	3.0	3.4	3.0	3.4
Charm-quark mass	1.2	1.5	1.2	1.5	1.2	1.5
Parton shower μ_F with heavy-flavour decorrelation	5.0	6.9	5.0	6.9	5.0	6.9
Parton shower PDF uncertainty	3.6	4.0	2.6	2.4	1.0	1.6
Angular coefficients	5.8	5.3	5.8	5.3	5.8	5.3
Total	15.9	18.1	14.8	17.2	11.6	12.9

W template systematic uncertainties

- Parton shower tuning is largely correlated between W and Z for light-quark initiated production
- Therefore Z PT tuning uncertainties are a suitable proxy for W PT modelling

- Heavy quarks participate differently for W and Z production, however.
- Independent QCD matching scales for charm and bottom quark in VFNS PDF evolution
- **Varying the heavy scales independently from the light quark ISR scale leads to 5-7 MeV MW shift**
- More extreme decorrelation of W and Z scales can lead to much larger shifts (up to 30 MeV!)
- There is no popular theory prescription for this. **Direct W PT modelling** will be an important ingredient of future measurements.

W-boson charge	W^+		W^-		Combined	
Kinematic distribution	p_T^ℓ	m_T	p_T^ℓ	m_T	p_T^ℓ	m_T
δm_W [MeV]						
Fixed-order PDF uncertainty	13.1	14.9	12.0	14.2	8.0	8.7
AZ tune	3.0	3.4	3.0	3.4	3.0	3.4
Charm-quark mass	1.2	1.5	1.2	1.5	1.2	1.5
Parton shower μ_F with heavy-flavour decorrelation	5.0	6.9	5.0	6.9	5.0	6.9
Parton shower PDF uncertainty	3.6	4.0	2.6	2.4	1.0	1.6
Angular coefficients	5.8	5.3	5.8	5.3	5.8	5.3
Total	15.9	18.1	14.8	17.2	11.6	12.9

MZ as a test case

- In Z events, one lepton can be ignored, as a neutrino, and the W mass measurement technique performed.
- Best-fit templates to PT, MT agree with data
- Best-fit MZ agrees with LEP 1 measurement

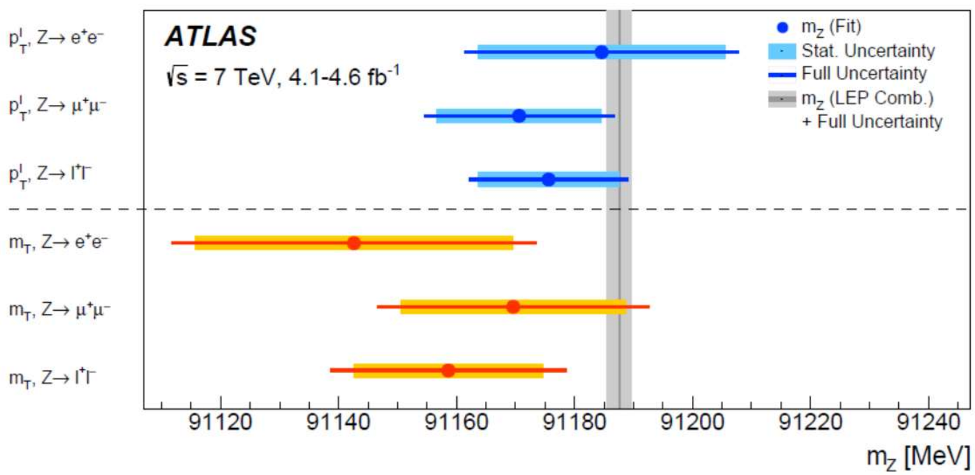

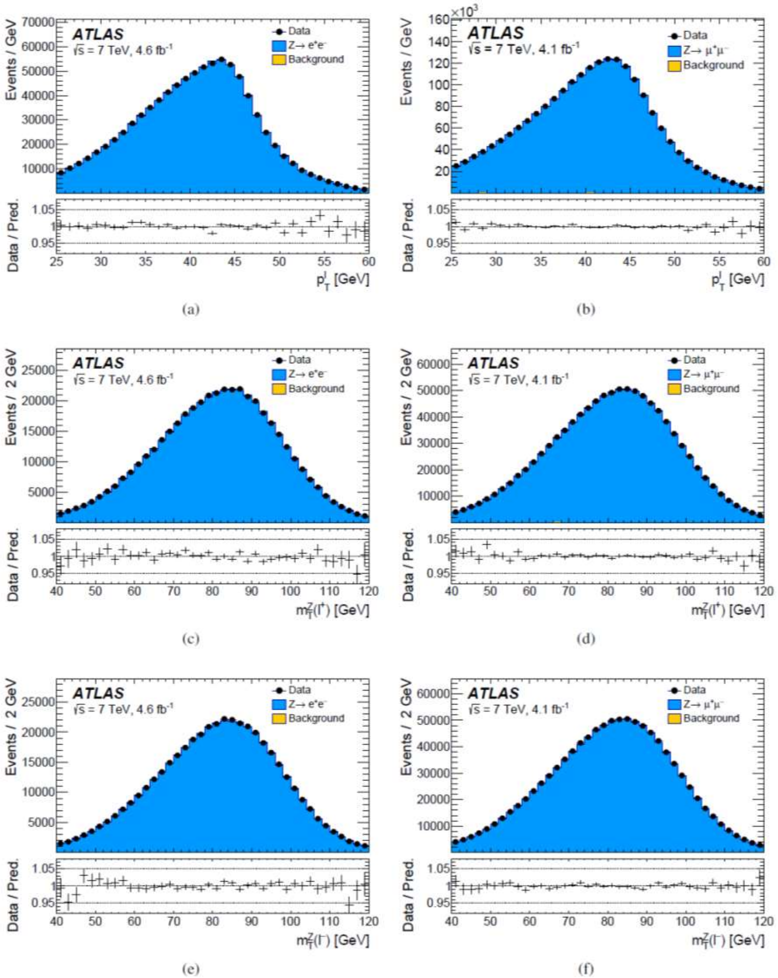

W fit results: data vs. post-fit model

W+ → μ+ν | W- → μ−ν | W+ → e+ν | W- → e−ν

PT

MT

PTmiss

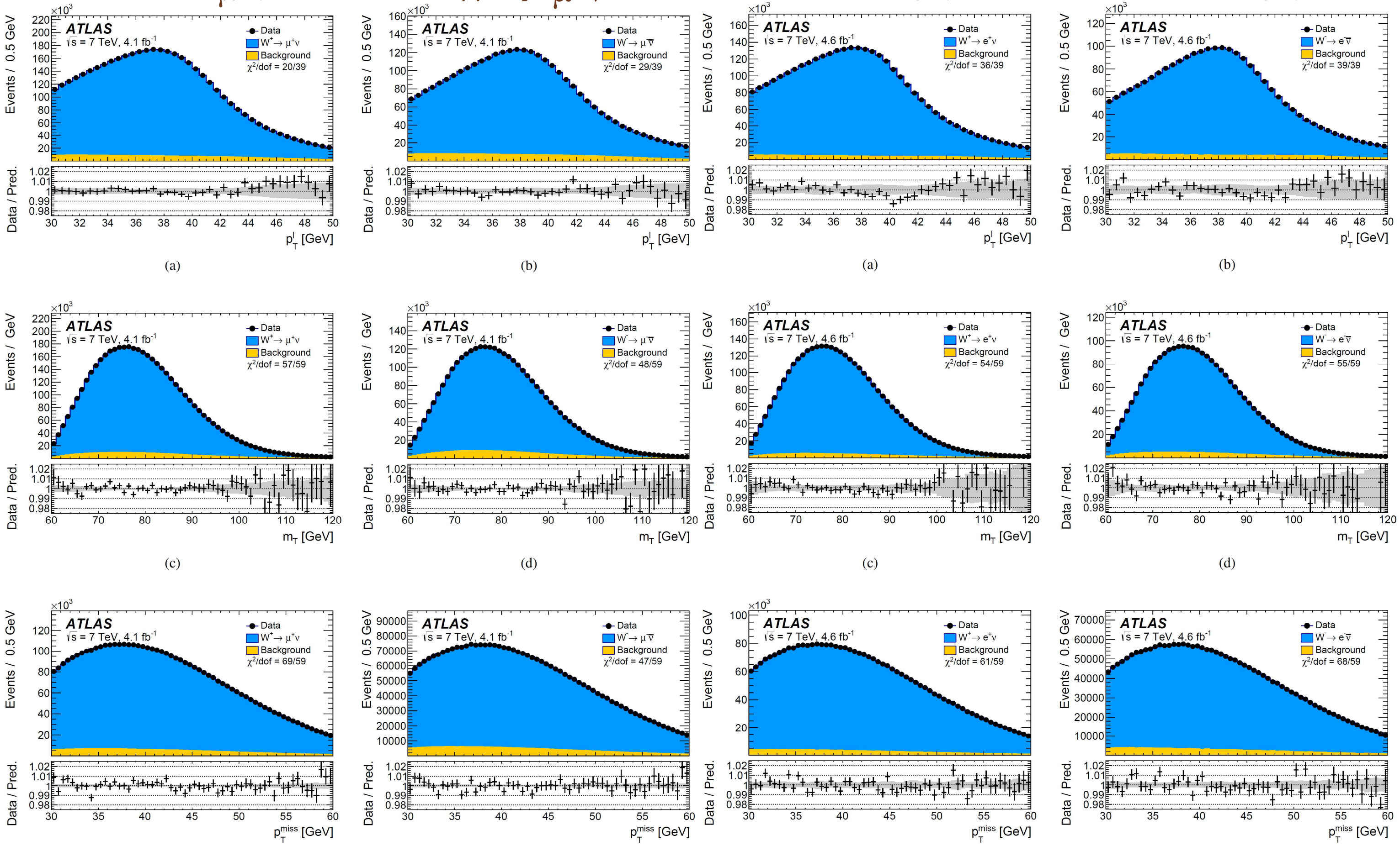

W fit results: by category

N.B. PT and MT results are ~50% correlated

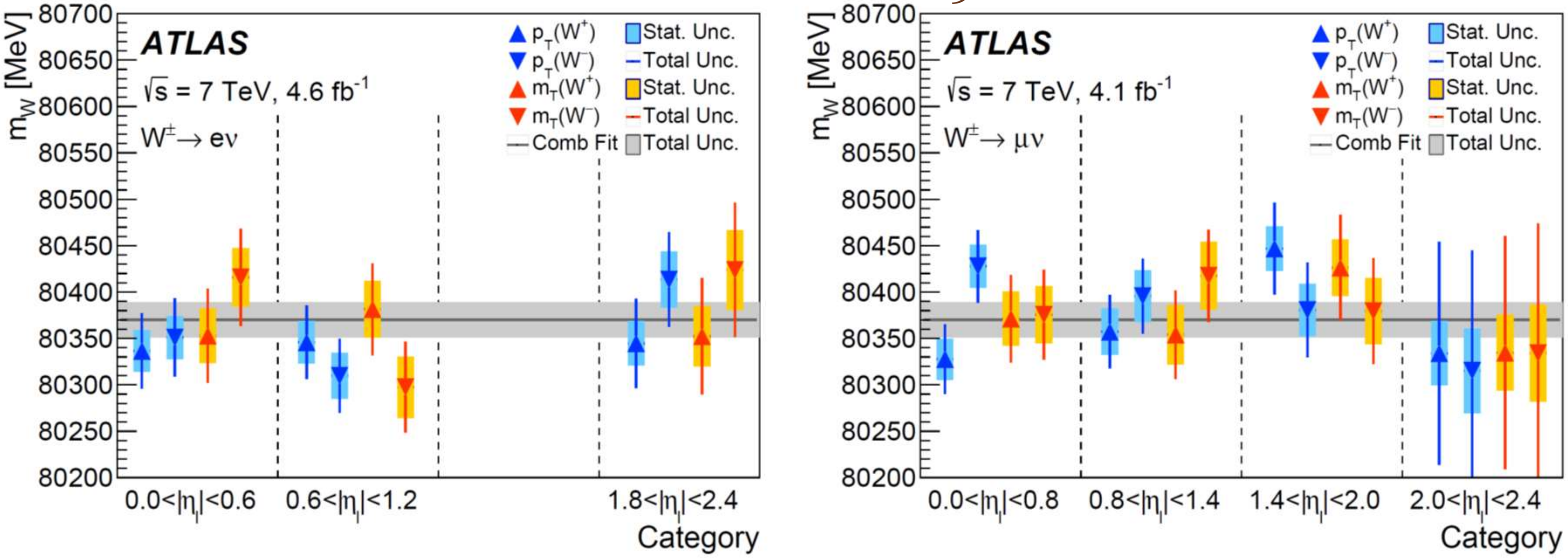

No bias trend in + vs. -, MT vs. PT, e vs. mu, or rapidity

W fit results: MT uncertainties

High-rapidity muons have larger momentum unc.

High-rapidity electrons have larger momentum and bkg. unc.

Channel m_T-Fit	m_W [MeV]	Stat. Unc.	Muon Unc.	Elec. Unc.	Recoil Unc.	Bckg. Unc.	QCD Unc.	EW Unc.	PDF Unc.	Total Unc.
$W^+ \to \mu\nu, \|\eta\| < 0.8$	80371.3	29.2	12.4	0.0	15.2	8.1	9.9	3.4	28.4	47.1
$W^+ \to \mu\nu, 0.8 < \|\eta\| < 1.4$	80354.1	32.1	19.3	0.0	13.0	6.8	9.6	3.4	23.3	47.6
$W^+ \to \mu\nu, 1.4 < \|\eta\| < 2.0$	80426.3	30.2	35.1	0.0	14.3	7.2	9.3	3.4	27.2	56.9
$W^+ \to \mu\nu, 2.0 < \|\eta\| < 2.4$	80334.6	40.9	112.4	0.0	14.4	9.0	8.4	3.4	32.8	125.5
$W^- \to \mu\nu, \|\eta\| < 0.8$	80375.5	30.6	11.6	0.0	13.1	8.5	9.5	3.4	30.6	48.5
$W^- \to \mu\nu, 0.8 < \|\eta\| < 1.4$	80417.5	36.4	18.5	0.0	12.2	7.7	9.7	3.4	22.2	49.7
$W^- \to \mu\nu, 1.4 < \|\eta\| < 2.0$	80379.4	35.6	33.9	0.0	10.5	8.1	9.7	3.4	23.1	56.9
$W^- \to \mu\nu, 2.0 < \|\eta\| < 2.4$	80334.2	52.4	123.7	0.0	11.6	10.2	9.9	3.4	34.1	139.9
$W^+ \to e\nu, \|\eta\| < 0.6$	80352.9	29.4	0.0	19.5	13.1	15.3	9.9	3.4	28.5	50.8
$W^+ \to e\nu, 0.6 < \|\eta\| < 1.2$	80381.5	30.4	0.0	21.4	15.1	13.2	9.6	3.4	23.5	49.4
$W^+ \to e\nu, 1,8 < \|\eta\| < 2.4$	80352.4	32.4	0.0	26.6	16.4	32.8	8.4	3.4	27.3	62.6
$W^- \to e\nu, \|\eta\| < 0.6$	80415.8	31.3	0.0	16.4	11.8	15.5	9.5	3.4	31.3	52.1
$W^- \to e\nu, 0.6 < \|\eta\| < 1.2$	80297.5	33.0	0.0	18.7	11.2	12.8	9.7	3.4	23.9	49.0
$W^- \to e\nu, 1.8 < \|\eta\| < 2.4$	80423.8	42.8	0.0	33.2	12.8	35.1	9.9	3.4	28.1	72.3

W mass consistency checks

- Consistent partial and full combinations for each channel/measurement

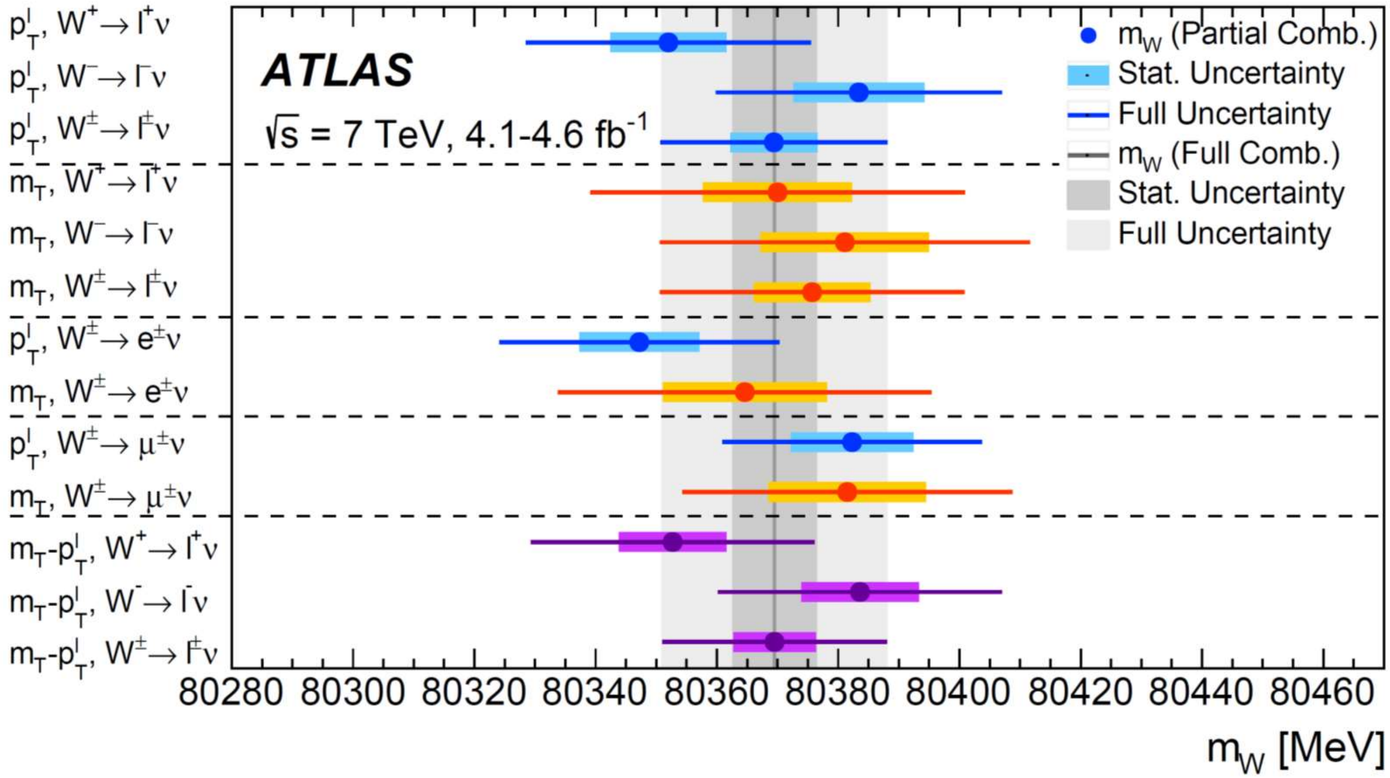

$$
\begin{aligned}
m_W &= 80369.5 \pm 6.8 \text{ MeV(stat.)} \pm 10.6 \text{ MeV(exp. syst.)} \pm 13.6 \text{ MeV(mod. syst.)} \\
&= 80369.5 \pm 18.5 \text{ MeV},
\end{aligned}
$$

W mass consistency checks

- PT and MT ranges are scanned

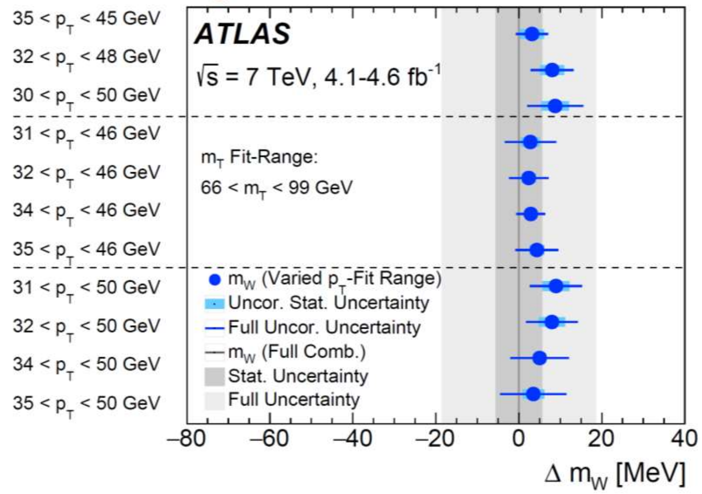

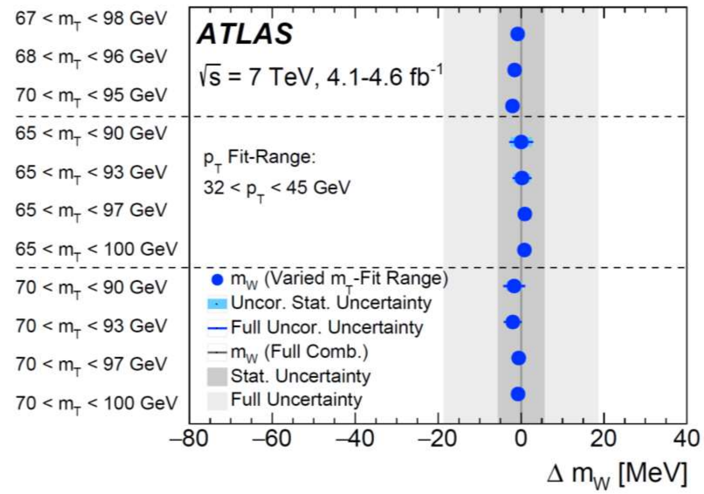

- Categories of pileup, uT, u||, and excluding the Ptmiss cut are also tested separately

Decay channel	$W \to e\nu$		$W \to \mu\nu$		Combined	
Kinematic distribution	p_T^ℓ	m_T	p_T^ℓ	m_T	p_T^ℓ	m_T
Δm_W [MeV]						
$\langle\mu\rangle$ in [2.5, 6.5]	8 ± 14	14 ± 18	-21 ± 12	0 ± 16	-9 ± 9	6 ± 12
$\langle\mu\rangle$ in [6.5, 9.5]	-6 ± 16	6 ± 23	12 ± 15	-8 ± 22	4 ± 11	-1 ± 16
$\langle\mu\rangle$ in [9.5, 16]	-1 ± 16	3 ± 27	25 ± 16	35 ± 26	12 ± 11	20 ± 19
u_T in [0, 15] GeV	0 ± 11	-8 ± 13	5 ± 10	8 ± 12	3 ± 7	-1 ± 9
u_T in [15, 30] GeV	10 ± 15	0 ± 24	-4 ± 14	-18 ± 22	2 ± 10	-10 ± 16
$u_\parallel^\ell < 0$ GeV	8 ± 15	20 ± 17	3 ± 13	-1 ± 16	5 ± 10	9 ± 12
$u_\parallel^\ell > 0$ GeV	-9 ± 10	1 ± 14	-12 ± 10	10 ± 13	-11 ± 7	6 ± 10
No p_T^{miss}-cut	14 ± 9	-1 ± 13	10 ± 8	-6 ± 12	12 ± 6	-4 ± 9

W mass results

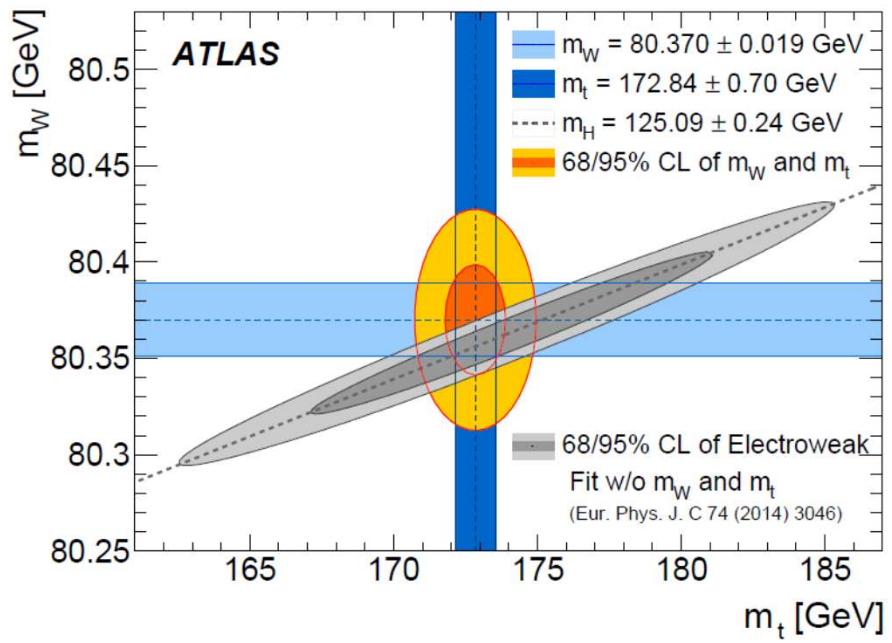

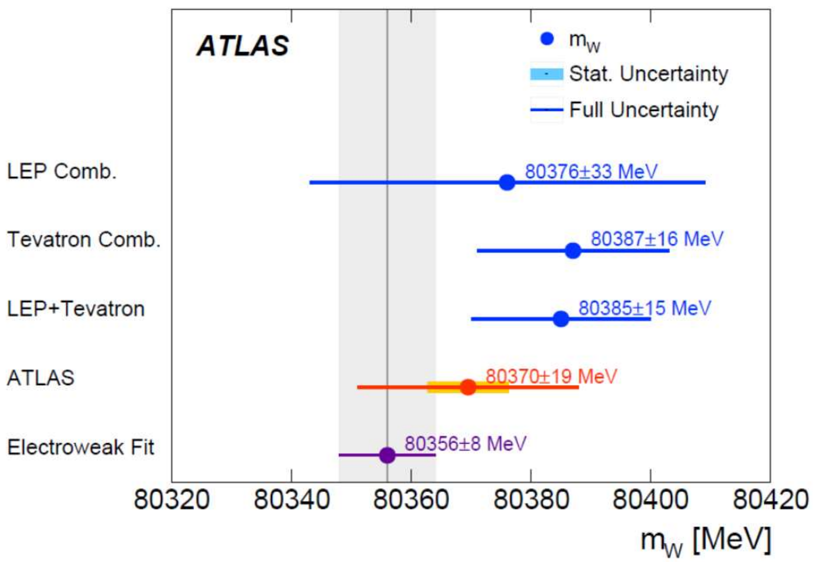

- The initial ATLAS measurement is about 25% less precise than the world average.
- It is consistent with the world average and a bit closer to the indirect Electroweak Fit prediction.

W mass uncertainty analysis and outlook

p_T-Fit	m_W [MeV]	Stat. Unc.	Muon Unc.	Elec. Unc.	Recoil Unc.	Bckg. Unc.	QCD Unc.	EW Unc.	PDF Unc.	Total Unc.
$W^+ \to \mu\nu, \lvert\eta\rvert < 0.8$	80327.7	22.1	12.2	0.0	2.6	5.1	9.0	6.0	24.7	37.3
$W^+ \to \mu\nu, 0.8 < \lvert\eta\rvert < 1.4$	80357.3	25.1	19.1	0.0	2.5	4.7	8.9	6.0	20.6	39.5
$W^+ \to \mu\nu, 1.4 < \lvert\eta\rvert < 2.0$	80446.9	23.9	33.1	0.0	2.5	4.9	8.2	6.0	25.2	49.3
$W^+ \to \mu\nu, 2.0 < \lvert\eta\rvert < 2.4$	80334.1	34.5	110.1	0.0	2.5	6.4	6.7	6.0	31.8	120.2

- In this design, leading uncertainties are statistical and PDF
- Improved **external or simultaneous PDF constraint** will improve future measurements
- But PDF uncertainties will be larger at 13 TeV

- Lepton momentum scale, which will tend to improve with more data and more sophisticated modelling

- QCD modelling uncertainties will likely best improve via semi-empirical methods (direct W PT measurement, e.g.) coupled with theory improvements

Conclusions for Lecture 2

- After decades of chasing Mt and MH, different fundamental parameters come into focus in order to tighten the electroweak vise of constraints on new physics.
- Copious W and Z data statistics can be traded in to eliminate a lot of the theory modelling systematics.
- In situ studies of detector performance can also evolve with statistics to improve energy scales and resolution.
- PDFs and low PT phenomenology need to be aggressively tuned by the data, either beforehand or simultaneously.
- **Which one will crack first??**

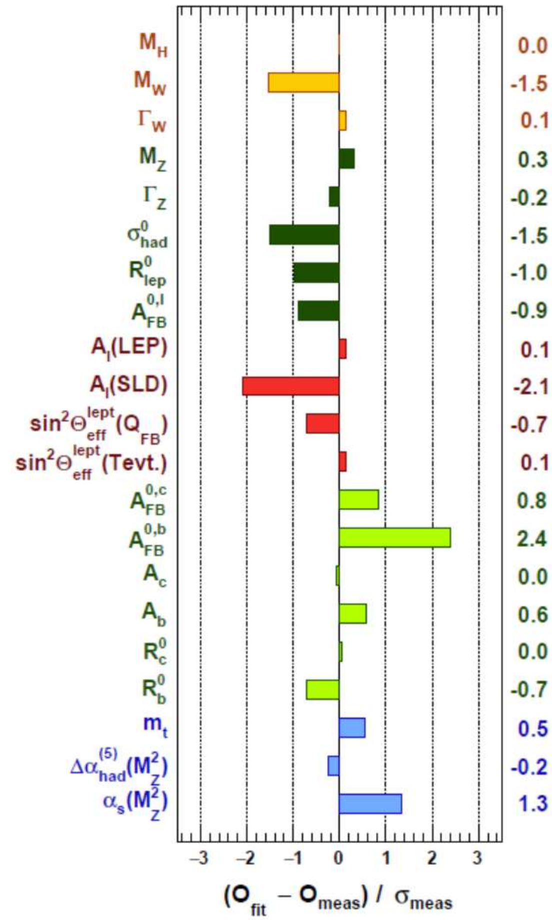

Syllabus: Review of six measurements

- Lecture 1, Friday Aug. 24
- The miracle of QCD: jets, tops, and α_S
- Lecture 2, Sunday Aug. 26
- The vise of precision electroweak: $\sin^2\theta_W$ and M_W
- Lecture 3, Monday Aug. 27
- The mystery of flavor: Capturing Wilson coefficients and testing lepton universality

References

- gFitter 2018 update arxiv:1803.01853
- ATLAS weak-mixing angle at 8 TeV ATLAS-CONF-2018-037
- ATLAS W mass at 7 TeV arxiv:1701.07240
- ATLAS Run 1 electron/photon calibration arxiv:1407.5063
- ATLAS Run 1 muon performance arxiv:1407.3935